Institut für Pharmakologie und Toxikologie
der Techischen Universität München

Distribution and Characterisation of Novel Voltage Gated Calcium Channel Subunits

Elsé Marais

Vollständiger Abdruck der von der Fakultät Wissenschaftszentrum Weihenstephan für Ernährung, Landnutzung und Umwelt der Technischen Universität München zur Erlangung des akademischen Grades eines

Doktors der Naturwissenschaften

genehmigten Dissertation.

Vorsitzender: Univ-Prof. Dr. K-H Schleifer

Prüfer der Dissertation:

1. Univ-Prof. Dr. W. Staudenbauer
2. Univ-Prof. Dr. F. Hofmann

Die Dissertation wurde am 29 Januar 2001 bei der Technischen Universität München eingereicht und durch die Fakultät Wissenschaftszentrum Weihenstephan für Ernährung, Landnutzung und Umwelt am 19 März 2001 angenommen.

Abbreviations

ATP	adenosine-5'-triphosphate
BSA	bovine serum albumin
cAMP	cyclic AMP
cDNA	complementary DNA
C.elegans	*Caenorhabditis elegans*
Ci	Curie (1 Ci = $3.7x10^{10}$ Bq)
CIP	calf intestinal phosphatase
COS-7	African green monkey kidney cells
CTP	cytosine-5'-triphosphate
cpm	counts per minute
Da	Dalton
DHP	dihydropyridine
DMEM	Dulbecco's MEM
DMSO	dimethylsulfoxide
DNA	deoxyribonucleic acid
dNTP	2'deoxynucleoside-5'-triphosphate
DTT	dithiotreitol
E. coli	*Escherichia coli*
EDTA	ethylenediamine tetra-acetic acid
EGTA	ethylene-bis (oxyethylenenitrilo)-tetra-acetic acid
FCS	foetal calf serum
GABA	γ-amino butyric acid
GBP	gabapentin
GTP	guanosine-5'-triphosphate
HEK293	human embryonic kidney cells
hr	hours
HEPES	2-[4-(-2-hydroxyethyl)-1-piperazino]ethane sulfonic acid
IC_{50}	50% inhibitory concentration
ISH	*in situ* hybridisation
K_d	dissociation constant
LB	Luria Bertani medium
MEM	minimal essential medium
min	minute
MOPS	γ-morpholino-propane sulfonic acid
NMDA	N-methyl-D-aspartate
nt	nucleotide
OD	optical density
PAGE	polyacrylamide gel electrophoresis
PCR	polymerase chain reaction
PEG	polyethylene glycol
RNA	ribonucleic acid
RNase	ribonuclease
rpm	revolutions per minute
SDS	sodium dodecyl sulphate
s	second
SEM	standard error of the mean
ssDNA	single stranded DNA
TEMED	N,N,N',N'-tetramethylethylenediamine
Tris	Tris-(hydroxymethyl)-aminomethane
tRNA	transfer RNA
TTP	thymidine-5'-triphosphate
U	unit
UV	ultraviolet

1 Introduction

The transfer of ions such as Na^+, K^+ and Ca^{2+} across membranes is a fundamental process of information transfer in cells. Ions are transferred across the bilipid membrane by channels, which are proteins that form a pore through which the ions can move. The essential properties that underlie the signalling ability of channels is their ionic specificity, their ability to be regulated and the kinetics of the opening and closing of the pores.

1.1 Calcium channels

The influx of calcium ions couples electrical activity with intracellular signal transduction, thereby playing a pivotal role in the triggering and modulation of cell excitability and function. Calcium ions are second messengers that regulate processes as diverse as hormone secretion, pacemaker activity, smooth muscle contraction and neurotransmission. The flow of calcium through the plasma membrane is regulated by a large family of channels, which open and close in response to an appropriate stimulation. This stimulus can take the form of interactions between pore proteins and cyclic nucleotides, binding of neurotransmitters to channel receptors or changes in the potential difference across the membrane. The latter form of calcium channels, known as voltage activated calcium channels, activate upon membrane depolarization caused by action potentials as well as sub-threshold depolarization signals.

A number of voltage gated calcium channels exist, which can be broadly classed as High Voltage Activated (HVA) and Low Voltage Activated (LVA) channels. HVA channels have large single channel conductance and variable voltage dependent inactivation. These channels are regulated by cAMP-dependent protein phosphorylation and are inhibited by drugs such as dihydropyridines (DHP), phenylalkylamines and benzothiazepines. LVA channels are activated at more negative potentials, inactivate rapidly and have small single channel conductance. The HVA channels can be sub-grouped into L-, R-, P/Q and N-type, depending on their biophysical characteristics. Both HVA and LVA channels consist at least of an α_1 pore protein that conducts current, is the target of drugs and contains the voltage sensor. A change in conformation of the pore protein is induced by a physical shift of the voltage sensor, effectively opening the channel and allowing calcium ions to enter the cell. Closing of the pore occurs as the calcium channel inactivates, a process triggered by the

decrease in the electrochemical driving force, as well as intrinsic shut-down mechanisms that prevent excessive influx of calcium.

The first voltage gated calcium channel was purified and cloned from transverse tubules of skeletal muscle (Curtis and Catterall 1984, Takahashi et al. 1987) and found to consist of α_1, α_2, δ, β and γ subunits (reviewed in Suh-Kim et al. 1996). Since then a total of seven genes have been identified for the α_1 pore subunits of HVA channels (for a review see Hofmann et al. 1999) and three for LVA channels (Perez-Reyes et al., 1998, Cribbs et al. 1998, Lee et al. 1999). The calcium channel α_1 proteins are 190-250kDa large and consist of 4 similar structural domains. These domains are predicted to have 6 transmembrane segments, with a membrane-associated loop between segments 5 and 6 forming the pore. Although the subunits were originally named according to the tissue in which they were identified, eg. α_{1S} from skeletal muscle, a new nomenclature based on relatedness and shared characteristics has recently been adopted (shown below). The $Ca_v1.1$-4 α_1 subunits are classified as L-type, dihydropyridine (DHP) sensitive HVA channels, and the $Ca_v2.1$-3 sub-group as non-DHP sensitive HVA channels. The LVA channels form the third group, $Ca_v3.1$-3.

Old nomenclature	**Current type**	**Drug sensitivities**	**Distribution**	**New nomenclature**
α_{1S}	L	DHP	Skeletal muscle	$Ca_v1.1$
α_{1C}	L	DHP	Heart, smooth muscle, brain	$Ca_v1.2$
α_{1D}	L	DHP	Brain, endocrine tissues, cochlea	$Ca_v1.3$
α_{1F}	L		Retina	$Ca_v1.4$
α_{1A}	P/Q	ω-agatoxin IVA	Brain, peripheral nervous system	$Ca_v2.1$
α_{1B}	N	ω-conotoxin GVIA	Brain	$Ca_v2.2$
α_{1E}	R	SNX-482, -ACN, -ECN	Brain, retina, endocrine tissues, heart, cochlea	$Ca_v2.3$
α_{1G}	T	Mibefradil, kurtoxin	Brain, heart	$Ca_v3.1$
α_{1H}	T	Mibefradil, kurtoxin	Heart, brain, kidney	$Ca_v3.2$
α_{1I}	T	Mibefradil	Brain	$Ca_v3.3$

1.2 Neuronal calcium channels

Voltage activated calcium channels are fundamental to neuronal function. Of the known α_1 subunits, only $Ca_v1.1$ and $Ca_v1.4$ are not found in brain. The L-type channels, $Ca_v1.2$ and $Ca_v1.3$, are postulated to be associated with NMDA receptors and to play an important role in the coupling of excitation to gene transcription. These channels are therefore not required for fast synaptic transmission, but for longer term signal transduction.

N- and P/Q type channels are found in presynaptic nerve terminals (Westenbroek et al. 1992, Westenbroek et al. 1995), and are thought to be involved in excitation-secretion coupling. Exocytosis of synaptic vesicles requires high Ca^{2+} concentrations, and the channels directly interact with the synaptic vesicle docking and fusion machinery (Catterall 1998). These interactions are calcium dependent, channel specific and regulated by phosphorylation. T-type current, ie. the $Ca_v3.1$-3.3 subunits, are responsible for neural behaviour that is triggered near the resting potential, such as thalamic oscillations and rebound burst firing (Huguenard 1998).

While it is known that HVA channels are modulated by accessory subunits physically associated with the α_1 pore, it remains to be unequivocally established whether the LVA channels are similarly structured. The HVA auxiliary subunits are the β, $\alpha_2\delta$ and γ proteins (Figure 1).

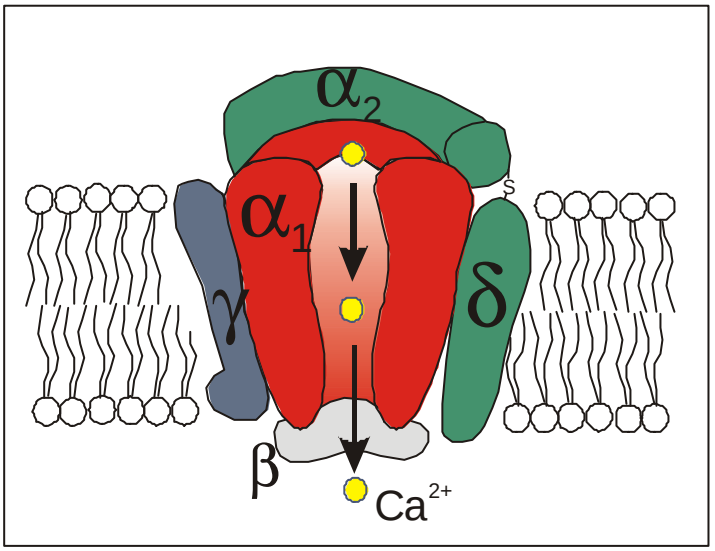

Figure 1: A schematic representation of a High Voltage Activated channel, consisting of an α_1 pore protein and the auxiliary β, γ and $\alpha_2\delta$ subunits.

1.3 The b and g auxiliary subunits

The β subunits are cytosolic proteins of 52-78kDa that chaperone α_1 to the cell surface and remain associated with the pore. These subunits modulate all aspects of HVA channel function such as the current amplitude, rate and voltage dependency of activation and inactivation, coupling of voltage sensing to pore opening, relief from G-protein inhibition and ligand binding (for review see Birnbaumer et al. 1998). Four non-allellic genes have been identified for the subunit (Ruth et al. 1989, Perez-Reyes et al. 1992, Hullin et al. 1992, Castellano and Perez-Reyes 1993) as well as multiple splice variants. The proteins and their splice forms are expressed in a tissue-specific manner. The effect of the β subunit on channel function varies according to the β and α_1 type. In some cases the β's can be 'reshuffled' to compensate to some extent for the absence of one of the subunits. This is seen with β4, where a mutation causes a premature termination of the protein, producing the neurological deficits in so-called lethargic mice (Burgess et al. 1997). However, knocking out the β1 gene in mice leads to death at birth (Gregg et al. 1993).

Until recently only a single, skeletal muscle specific γ subunit had been identified (Jay et al. 1990). Mice with absence epilepsy (stargazer phenotype) were subsequently found to have an early transposon inserted into a homologous gene, which was named γ2 (Letts et al. 1998). This new family member was found to be brain specific, and although some functional mRNA may be produced, the transposon insertion causes considerable phenotypic aberrations. In addition to γ2, three other γ subunits have recently been identified in mouse (Klugbauer et al. 2000). Two homologs were also identifed in human, as well as a sixth γ subunit that has not yet been further characterised (Black et al. 1999, Burgess et al. 1999). γ3 and γ4 are also only found in brain, whereas γ5 is expressed in kidney, skeletal muscle, liver and lung (Klugbauer et al. 2000). The sequence identity between γ1 and the rest of the family is low, with γ1 and γ2 only 25% related at the amino acid level. A sequence alignment is shown in Figure 20. The hydrophobicity profiles are similar however and several structural motifs are conserved. The neuronal γ's are 60% identical, and form a phylogenetic subgroup.

The γ subunits are 35-38kDa proteins with 4 putative transmembrane segments and cytosolic amino and carboxy termini. The γ1 subunit modulates the peak current as well as the activation and inactivation kinetics of the skeletal muscle α_1 subunit (Eberst et al. 1997, Singer et al. 1991). In a γ1

mouse knock-out model, the calcium influx was decreased relative to controls, and the steady state inactivation shifted to more positive potentials (Freise et al. 2000). The electrophysiological effects of γ2 on the neuronal $Ca_v2.1$ subunits are modest, with a 7mV hyperpolarizing shift of the voltage dependence of activation (Letts et al. 1998). This may be enough to lead to an increased calcium current that disturbs the neuronal firing patterns.

1.4 The $\alpha_2\delta$ auxiliary subunit

The $\alpha_2\delta$ family consists of three genes. The first subunit identified was $\alpha_2\delta$-1 in rabbit skeletal muscle (Ellis et al., 1988) together with the first α_1, β and γ subunits. Five tissue-specific $\alpha_2\delta$-1 splice variants exist (Angelotti and Hofmann, 1996) but a functional significance of the splicing has not been established. Two new $\alpha_2\delta$ family members were subsequently identified in human and mouse, and were named $\alpha_2\delta$-2 and -3 (Klugbauer et al., 1999a). The novel $\alpha_2\delta$ subunits are 56 and 30% homologous to $\alpha_2\delta$-1 at the amino acid level and share a number of structural motifs. Only a single $\alpha_2\delta$-3 splice form was found, but two splice variants differing by a total of 7 amino acids were identified for $\alpha_2\delta$-2. All three $\alpha_2\delta$'s have similar hydrophobicity profiles and contain several potential N-glycosylation sites. An alignment of the subunits is shown in the appendix (7.1).

$\alpha_2\delta$-1 consists of 2 proteins – a highly glycosylated α_2 that is believed to be extracellularly located, and a smaller δ protein that anchors the α_2 to the cell membrane (Brickley et al. 1995; Wiser et al., 1996). These proteins are coded for by a single gene, the product of which is translated as a precursor polypeptide that is post-translationally cleaved (De Jongh et al., 1990). The α_2 and δ associate by disulfide bridges that form between the numerous cysteine residues found in both proteins (Figure 2). The characteristics of the novel $\alpha_2\delta$ have until now not been established.

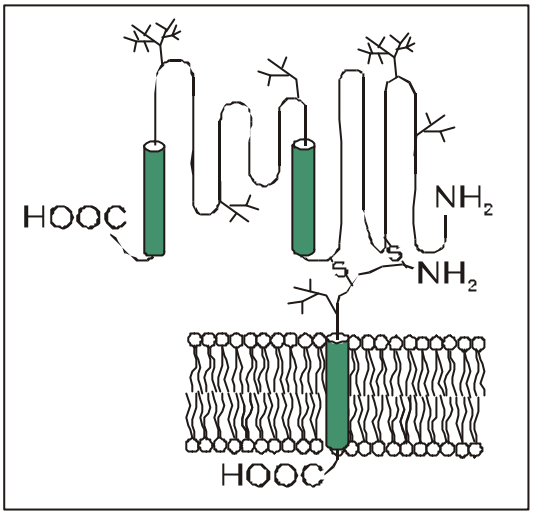

Figure 2**:** Line drawing of the $\alpha_2\delta$-1 subunit. Although the α_2 has 2 hydrophobic domains, it is believed to be entirely extracellular. The α_2 is bound to the transmembrane δ by disulfide bridges. Both proteins are glycoslyated.

The effects of $\alpha_2\delta$-1 on the biophysical properties of α_1 subunits depend on the expression system and subunits used. $\alpha_2\delta$-1 invariably increases the current density of calcium channels by increasing the amount of functional channel at the cell surface, and has been reported to allosterically alter the activation and inactivation of several α_1 subunits (Singer et al., 1991; Bangalore et al.; 1996, Felix et al., 1997; Klugbauer et al., 1999a). $\alpha_2\delta$-1 is also known to enhance DHP binding to L-type channels and ω-conotoxin GVIA to N-type channels (Felix et al., 1997; Brust et al., 1993). Co-expression experiments with β2a subunit and $\alpha_2\delta$-1 show that these auxiliary subunits have a co-operative effect on the expression of the $Ca_v1.2$ (α_{1C}) channel at the membrane, resulting in an increase in current density (Yamaguchi et al 2000).

The molecular diversity of voltage gated calcium channels is due to the expression of several forms of the subunit proteins, as well as differential splicing of the mRNA. The existence of these numerous forms allows for many different pore-accessory protein combinations, which may be one way in which temporal and tissue specific control is exercised over calcium entry. Mutations of several channel proteins have been shown to be causative factors in several disorders, making the calcium channel subunits targets for therapeutic interventions (Burgess and Noebels, 1999).

1.5 Gabapentin

Gabapentin (1-(aminomethyl)cyclohexane acetic acid) is an anti-epileptic drug that was originally designed as an analog to the inhibitory neurotransmitter, GABA (Leiderman 1994). It penetrates the blood-brain barrier through the L-system amino acid transporter and is well tolerated (McLean 1995) (Figure 3). Although structurally similar to GABA, gabapentin (GBP) was initially not found to bind any GABA receptors (Suman-Chauhan et al. 1993). However, there is evidence for GBP acting as an agonist of a specific population of $GABA_B$ receptors in hippocampal neurons (Ng et al., 2001). These receptors are G-protein coupled proteins that bind GABA and decrease neuronal excitability postsynaptically by activating inwardly rectifying K^+ conductance. In addition to its use against epilepsy, GBP is increasingly finding application in pain and anxiolytic disorders (Beydoun et al., 1995; Welty et al., 1993). GBP binds to rat brain (Suman-Chauhan et al. 1993; Hill et al. 1993) and skeletal muscle homogenates (Gee et al., 1996), with lower binding seen in heart, lung and pancreas (Suman-Chauhan et al., 1993). This binding was found to be due to the specific interaction of GBP with the $\alpha_2\delta$-1 subunit of voltage activated calcium channels (Gee et al., 1996). Since voltage activated channels are involved in controlling the electrical excitability of neurons, it has been postulated that this drug reduces calcium current by modulating α_1 indirectly through its association with $\alpha_2\delta$-1 (Gee et al 1996, Taylor 1998). Whether the clinical effects of GBP are due to calcium channel modulation, $GABA_B$ receptor interactions, or a combination of both, remains to be established.

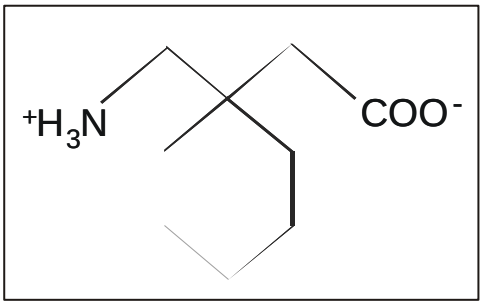

Figure 3: Structure of gabapentin (GBP), a drug used for neurological disorders. The $\alpha_2\delta$-1 subunit is known to bind GBP.

The identification and characterisation of calcium channel subunits is essential for understanding the contribution of the channels to cellular and organ function, as well for enabling the design of drugs to counter diseases associated with abnormalities in calcium influx.

2 Aim

Due to advances in molecular techniques, numerous voltage activated calcium channels subunits have been cloned and characterised. It is unclear however, which subunits associate to form the multi-protein channel complexes *in vivo*. Since the subunits differ in their conducting and modulatory properties, it is the combination of subunits making up the channel that defines the electrophysiological properties of the cell membrane. In our laboratory several novel subunits have recently been identified and cloned ($Ca_v3.1$, γ3, γ4, γ5, $\alpha_2\delta$-2 and $\alpha_2\delta$-3). It is therefore of interest to investigate how these novel, as yet uncharacterised subunits, associate. Such associations can be established using two complementary techniques. The distribution of subunit mRNA in brain can be determined by *in situ* hybridisation. An overlap of subunit expression may reflect physiological interactions, since the subunits are localised to the same cells. As a second approach, cDNA clones of the novel subunits can be expressed in a human cell line, and changes in the biophysical properties of the channels measured. This, together with the spatial distribution of the subunits, can be used to infer which proteins naturally interact.

Although the auxiliary $\alpha_2\delta$-1 subunit has been intensively studied, the distribution and properties of $\alpha_2\delta$-2 and -3, which were first identified in our laboratory, have not been investigated. Immunoblotting studies can be used to elucidate the gross protein structure of the novel $\alpha_2\delta$-2 and -3 subunits. It is of particular interest to determine whether the characteristic traits of $\alpha_2\delta$-1, namely its composition of two proteins derived from a single precursor protein, and its high level of glycosylation, are conserved in the new isoforms. Furthermore, since $\alpha_2\delta$-1 is known to bind the anti-epileptic drug gabapentin, it is also important to establish whether $\alpha_2\delta$-2 and $\alpha_2\delta$-3 are capable of drug binding.

3 Materials and Methods

The molecular and cell biological methods applied are described in this section. Techniques that are common to the larger analyses are presented first. The more complex methods, namely Northern blotting, *in situ* hybridisation, functional characterisation, immunoblotting and gabapentin binding assays, are subsequently described.

3.1 Materials

All reagents used were of molecular biology grade. The composition of specific solutions are given in the relevant methods, and general buffers are presented in section 3.20. Speciality items purchased are shown in Table 1.

Table 1: Suppliers of speciality materials.

Material	*Supplier*
pcDNA3 pcDNA3.1/Myc-His pcDNA3.1/V5/His-TOPO Zero blunt TOPO PCR cloning kit Anti-Myc monoclonal antibody	Invitrogen
Restriction enzymes T4 ligase T7 and T3 polymerase T4 DNA polymerase	New England Biolabs
E.coli XL1 blue MRF´	Stratagene
Anti-$\alpha_2\delta$-1 monoclonal antibody	Applied Bioregents
ABI Prism 310 Genetic Analyzer and Sequencing reaction kit	PE Applied Biosystems
Dulbecco's MEM MEM Lipofectamine	GIBCO Life Technologies
Human and Mouse multiple tissue northern blots Human Dot Blot	Clontech
DEPEX	SERVA

Material	*Supplier*
Sephadex G-50 Nick-columns ECL system Hybond ECL nitrocellulose Hyperfilm	Amersham Pharmacia
Random primed labelling kit N-glycosidase F FuGene 6	Roche
[^{3}H]-gabapentin	Custom synthesised by Amersham Pharmacia
NTB-2 photographic emulsion	Kodak
CY-3 conjugated goat anti-rabbit IgG Normal goat serum	Jackson Laboratories
Anti-mouse-horseradish peroxidase	Dianova
Centrisep size exclusion columns	Princeton Separations
Sulfolink coupling gel	Biorad

3.2 Vectors used

cDNA sequences were inserted into the vectors listed below for amplification, manipulation and expression in mammalian systems.

pcDNA3 is a eukaryotic expression vector that can be cultured in *E.coli*. pcDNA3 has a cytomegalovirus promoter for high level transcription of the inserted sequence, a polyadenylation signal and a transcription termination sequence.

pAL was constructed for *in vitro* transciption of RNA probes (Ludwig et al. 1997). T3 and T7 promoters with *Bam*HI and *Asp*718 sites were inserted into the multiple cloning site of the pUC19 vector. The promoters bind the T3 and T7 polymerases, allowing for transcription of the insert sequence. The restriction sites are used for the linearisation of the plasmid prior to transcription of the template DNA.

pcDNA3.1/V5/His-TOPO is a pcDNA3 based vector with attached vaccinia virus topoisomerase that aids the ligation of blunt-ended sequences. This vector was used for cloning of PCR products and blunt-ended inserts.

pcDNA3.1/Myc-His is a pcDNA 3 derived vector with a Myc-His fusion tag allowing for detection and purification of the fusion protein.

3.3 Bacterial techniques

3.3.1 *E.coli* culture and storage

The strain used for amplification of plasmid DNA was *E.coli* XL1 blue MRF´. The genotype is: Δ(*mrcA*)*183* Δ(*mrcCB-hsdSMR-mrr*)*173 endA1 supE44 thi-1 recA1 lac* [F' *proAB lacI*^{q}*ZDM15 Tn10* (Tet^{r})]. Culturing of *E.coli* was done in Luria-Bertani (LB) medium (3.20). The bacteria were grown in glass or polypropylene vessels at 37°C on a shaker set at 225rpm. Selective antibiotics included in the liquid media included ampicillin and kanamycin at 100µg/ml. Agar plates were prepared using LB medium and agar (15g/l). The medium was autoclaved, cooled to 55°C and antibiotics added. Plates containing 50µg/ml ampicillin were used with pCDNA3 and pcDNA3.1/Myc-His, and 50µg/ml kanamycin for pcDNA3.1/V5/His-TOPO. Cultured bacteria were plated onto agar plates, and following overnight incubation at 37°C, kept for short term storage at 4°C. For longer term storage glycerol stocks were prepared (1:1 bacterial culture:glycerol).

3.3.2 Preparation of competent bacteria

E.coli capable of taking up plasmid DNA were prepared as follows: A 6hr pre-culture of *E.coli* XL1 blue MRF´ in LB(-) (no glucose or antibiotics) was set up and innoculated into 100ml LB(-) for a 16hr culture. The culture was placed on ice when the OD_{600} reached 0.35 to 0.38. The bacteria were pelleted at 4 000g, resuspended in 15ml 1x TTS (10% polyethyleneglycol 3350, 50mM $MgCl_2$, 5% DMSO in LB(-) medium), aliquoted and shock frozen in a dry-ice/ethanol bath. Competent cells were stored at -80ºC.

3.3.3 Transformation of *E.coli*

Plasmid DNA was introduced into competent *E.coli* by adding the ligation reaction (3.5.4) to 400µl competent cells and incubating on ice for 30min. This mix was added to 2.6ml LB medium and incubated at 37ºC, 150rpm for 1hr. The bacteria were plated onto agar containing the corresponding selective antibiotic and incubated overnight at 37ºC. Colonies were picked, cultured and the plasmid DNA isolated by the 'mini-prep' procedure (3.7.1). The DNA was analysed for the presence and orientation of insert DNA.

3.3.4 Zero Blunt TOPO cloning

A rapid and selective method was used to clone PCR products and problematic inserts. The ligation reaction was considerably quicker than that of the conventional ligation (3.5.4). A 5µl reaction contained 0.5 to 4µl PCR product and 0.5µl pCR-Blunt II-TOPO vector. The mix was incubated at room temperature for 5min and the reaction stopped by addition of 1µl stop solution. The contents of a vial of One Shot TOP 10 cells was added to the ligation mix and incubated on ice for 30min. After a heat shock for 30s at 42°C the tube was incubated on ice for 2min. 250µl of SOC medium was added and the tube shaken horizontally at 37°C for 1hr. Two volumes (10µl and 50µl) of bacteria were plated onto LB plates containing 50µg/ml kanamycin and incubated overnight. Since the insertion of a sequence into the vector results in the disruption of a lethal gene (*ccd*B), a high cloning efficiency is obtained.

3.4 DNA and RNA techniques

3.4.1 Determination of nucleic acid concentration

The concentration of DNA and RNA was photometrically measured at 260nm, and calculated based on 1 OD_{260} correponding to 50µg/ml for DNA, and 40µg/ml for single stranded RNA. Nucleic acid purity was assessed by the A_{260}/A_{280} ratio.

3.4.2 Nucleic acid precipitation

DNA and RNA were precipitated from aqueous solutions using salt and alcohol. A 1/10 volume of 3.3M sodium acetate, pH5.2, and a 2.5 volume of ice-cold 100% ethanol, or 1 volume of isopropanol, were added to the solution. After 10min at -20ºC, the solution was centrifuged for 15min at 13 000g in a benchtop centrifuge cooled to 4ºC. The pellet was washed with 70% ethanol, dried and resuspended in water. All DNA and RNA preparations were stored at -20ºC or -80ºC.

3.4.3 Phenol-chloroform extraction

To remove contaminant protein, DNA and RNA solutions were extracted with a mixture of phenol/chloroform/isoamylalcohol (25:24:1). An equal volume of phenol-chloroform was added to an aqueous solution, vortexed and centrifuged at 13 000g for 5min. The upper aqueous layer containing the nucleic acids was transferred to a fresh tube. To remove any remaining phenol, a chloroform wash was performed.

3.4.4 Polymerase Chain Reaction (PCR)

PCR was used to generate in *situ* hybridisation templates, probes for Northern blotting and for alteration of sequences. A 50µl reaction typically contained:

25pmol of forward and reverse primers
0.2mM each dATP, dCTP, dGTP, dTTP
1X PCR Buffer (10mM Tris/HCl pH 8.3, 50mM KCl, 1.5mM $MgCl_2$)
50-100ng of cDNA or plasmid DNA
0.05U *Taq* or *Pfu* polymerase.

The cycling protocol used was as follows:

Initial denaturation: 94ºC, 1min

30-40 cycles of:

Denaturation: 94ºC, 1min

Primer annealing: 45-65ºC, 1min

Elongation: 72ºC, 30s-2min

The annealing temperature was varied according to the melting temperature of the primers. Elongation time depended on the length of the desired product, with 1min used for amplification of 1kb.

3.5 Enzymatic manipulations of DNA

Various enzymes were used to analyse DNA fragments, as well as to prepare the sequences for ligation to plasmid DNA. These procedures are described below.

3.5.1 Restriction

Restriction enzymes were used according to the supplier's instructions. A typical reaction consisted of a 20µl volume containing 1-3µg of DNA, 1 x reaction buffer (from supplier), and 100µg/ml BSA. The reaction was incubated at the temperature recommended (usually 37ºC) for times from 30min to overnight, depending on whether a qualitative or quantitative restriction was required.

3.5.2 Dephosphorylation

To prevent the re-ligation of linearised vector and to promote the insertion of the desired DNA fragment, it was necessary to dephosphorylate the 5' ends of the vector. This was achieved using calf intestinal phosphatase (CIP). Linearised plasmid was incubated with 1U CIP in 50mM Tris pH8.0 (or restriction buffer compatible with CIP) for 20min at 37ºC. The enzyme was heat-inactivated at 75ºC for 10min prior to ligation.

3.5.3 Blunt-ending and phosphorylation

For blunt-end ligation, nucleotide overhangs of both vector and insert were eliminated using 1.5U T4 DNA polymerase in the supplied or other compatible buffer, with 0.18mM dNTP's added. The

DNA was incubated for 40min at 37ºC and subsequently heat-inactivated at 75ºC for 10min. For the case that PCR products were being inserted, it was necessary to phosphorylate the 5' ends. This was done by incubation of the DNA with 20U polynucleotide kinase for 40min at 37ºC, followed by heat inactivation.

3.5.4 Ligation

Insertion of a DNA fragment was done by sticky-end (both vector and insert have compatible overhangs) or blunt-end ligation (the ends of vector and insert have no overhangs). Linearised, dephosphorylated vector (approximately 50fmol) was incubated with an excess of insert DNA (100fmol) in 1 x ligase buffer containing ATP, and 1U T4 DNA ligase at 16ºC for 6-16 hrs. The ligase mixture was subsequently used to transform bacteria (3.3.3).

3.6 Electrophoretic separation of DNA and RNA

DNA and RNA fragments were separated from other nucleic acids through polyacrylamide or agarose matrices. This was done to isolate the desired fragments as well as to assess the success of a reaction, for example the *in vitro* transcription of riboprobes for *in situ* hybridisation (3.11). Precautions to avoid RNase contamination were taken for all RNA work.

3.6.1 Agarose and polyacrylamide gel electrophoresis

Nucleic acids were separated by vertical polyacrylamide gel electrophoresis (PAGE) or horizontal submarine agarose gel electrophoresis. For fragments smaller than 1kb, a 5% polyacrylamide gel was used, and agarose gels of 0.7% to 2% for larger fragments. 1 x TBE was used as the gel and running buffer. Polyacrylamide gels were run at 250-290V and agarose gels at 100V. Ethidium bromide (0.5µg/ml) was included in agarose gels to allow for visualisation of the nucleic acids. Polyacrylamide gels were stained in an ethidium bromide solution after electrophoresis. The gels were viewed under UV light and bands of the correct size excised. The DNA was subsequently electroeluted (3.6.2) and precipitated (3.4.2).

3.6.2 Electroelution

DNA in gels slices was electroeluted in 1 x TBE buffer in dialysis tubing secured at both ends. The electroelution chamber was cooled on ice and a constant current of 145mA applied for 1-2hrs. After elution, the TBE in the tubing was transferred to a 1.5ml tube and the DNA precipitated.

3.7 Isolation of plasmid DNA

Following amplification of plasmid DNA in *E.coli*, the episomal DNA was extracted using a rapid method ('Mini-prep') to screen for clones with the correct insert and orientation. Clones with the desired insert were then re-cultured in a larger volume, and high quality DNA extracted using a 'maxi-prep' method.

3.7.1 'Mini-prep' isolation of DNA

A rapid protocol was used to isolate plasmid DNA from bacterial colonies. Single colonies were picked from agar plates, innoculated into 3ml of LB medium containing the suitable selective antibiotic and grown overnight at 37°C, 225rpm. The bacteria were pelleted by centrifugation (5 000g), resuspended in 125µl buffer P1 (50mM Tris-Cl, pH8.0, 10mM EDTA, 100µg/mlRNase A) and transferred to 1.5ml tubes. 125µl of lysis buffer P2 (200mM NaOH, 1% SDS) was added, and the tubes incubated at room temperature for 5min. The reaction was neutralised with 125µl cold P3 (3M potassium acetate, pH5.5) and incubated on ice for 15min. Genomic DNA and bacterial debris was pelleted at 13 000g for 15min at 4ºC. The plasmid DNA in the supernatant was precipitated using isopropanol.

3.7.2 'Maxi-prep' isolation of DNA

For the large scale production of good quality plasmid DNA, the Qiagen Plasmid Purification system was used. A bacterial colony known to contain the desired insert was pre-cultured for 6hrs in 3ml LB medium containing a selective antibiotic. 100ml of LB medium (containing antibiotic) was innoculated with pre-culture and grown overnight. The bacteria were pelleted at 6 000g, for 10min at 4°C and resuspended in 10ml cold P1 (buffer as used with mini-preps). 10ml of lysis buffer P2 was added and incubated for 5min at room temperature. The solution was neutralised with 10ml of P3 and incubated on ice for 20min. This lysate was ultracentrifuged at 70 000g for 30min at 4°C and

the supernatant decanted onto an anion exchange column equilibrated with buffer QBT (750mM NaCl, 50mM MOPS, pH 7.0, 15% isopropanol, 0.15% Triton X-100). The column was washed twice with 30ml buffer QC (1M NaCl, 50mM MOPS, pH 7.0, 15% isopropanol) and the DNA eluted with 15ml buffer QF (1.25M NaCl, 50mM Tris-Cl, pH 8.5, 15% isopropanol). The DNA was precipitated with 10.5ml isopropanol and pelleted at 10 000g (30min, 4°C). A 70% ethanol wash was performed, the pellet dried and resuspended in water.

3.8 DNA Sequencing

DNA preparations were sequenced using the ABI Prism 310 Genetic Analyzer and BigDye Terminator Cycle Sequencing Ready Reaction mix. A sequencing reaction consisted of 0.5µg plasmid DNA or 90ng purified PCR product, 3.2pmol primer and 5µl of Reaction Ready Mix in a 20µl volume. To incorporate the fluorescent nucleotides into the template, the reaction was cycled 25 times as follows:

Denaturation: 95ºC, 30s
Annealing: 50ºC, 50s
Elongation: 60ºC, 4min

Separation of template from unincoporated nucleotides was achieved by centrifugation through a Centrisep size-exclusion column, following the manufacturer's instructions. The eluted template was dried, resuspended in Template Suppression Reagent and denatured at 95ºC for 3min. The sample was then electrophoresed through short or long capillaries of the Genetic Analyzer and analysed with the supplied software.

3.9 Generation and purification of radioactively labelled probes

3.9.1 Random primed labelling

Radioactively labelled DNA fragments were generated using the Random Primed Labelling Kit. 25ng of template DNA was denatured at 100ºC for 10min and placed on ice. In a final volume of 20µl the following was added: 25mM each of dATP, dTTP and dGTP, 2µl 10X reaction buffer containing

random hexanucleotide primers, 2U of Klenow enzyme and 50µCi ^{32}P-dCTP. The reaction was incubated at 37ºC for 30min. The enzyme was inactivated at 65ºC for 10min before purification through a Nick column (3.9.2).

3.9.2 Purification of labelled oligonucleotides

A Sephadex G-50 Nick column was used to separate radioactively labelled DNA or RNA probes from unincorporated nucleotides. The column was equilibrated with 1 x TE, the sample loaded in a volume of 300µl TE, followed by 800µl of TE. Fractions were collected, and the elution profile followed by scintillation counting. The fraction containing the labelled probe was stored at -20ºC in the case of ^{32}P-labelling of DNA, or made up in hybridisation buffer in the case of ^{35}S-labelling of riboprobes, prior to storage at -20ºC.

3.10 Northern and dot blot analysis

The cDNA probe used for the $\alpha_2\delta$–1 dot blot was generated by PCR (3.4.4) using primers listed in section 7.3. This probe corresponded to nucleotides 2760-3170 of the rabbit clone. The $\alpha_2\delta$–2 and –3 probes were similarly generated, and correspond to nucleotides 2897-3249 and 2893-3377, respectively. Commercially available mouse and human multiple tissue Northern blots and dot blots were used. The membranes were pre-hybridised in 1ml/5cm^2 hybridisation buffer (1 x PE, 4 x SSC, 50% formamide, 150µg ssDNA) at 65°C for 3hrs. The solution was replaced with fresh buffer containing 5x10^6 cpm/ml of ^{32}P-labelled probe (3.9.1) that had been denatured for 10min at 100°C, and the blot incubated overnight at 42°C. To remove excess and non-specifically bound probe, the blot was washed twice for 5min with 2 x SSC, 0.1% SDS at room temperature, twice for 10min with 1 x SSC, 0.1% SDS at room temperature and finally with 0.1 x SSC, 0.1% SDS at temperatures up to 60°C. The blot was exposed to Hyperfilm at -80°C for several hours to days and developed in an automated film developer.

3.11 In Situ Hybridisation (ISH)

In order to study the physiological distribution of various calcium channel subunits, their mRNA expression patterns were determined by hybridising antisense riboprobes to cryosections of mouse brain.

3.11.1 Preparation of brain slices

Wild-type Balb/C mice were killed by cervical dislocation. Intact brains were removed immediately following death and frozen in isopentane cooled to -40°C in a dry-ice/ethanol bath. The brains were sectioned at 16µm in a cryostat and thaw mounted onto polylysine slides. The tissue was vacuum dried for 30min, fixed in 4% paraformaldehyde in PBS (20min) and washed in 1 x PBS (5min). Sections were acetylated in 0.25% acetanhydride in 0.1M triethanolamine-HCl, pH 8.0, for 10min and washed in 2 x SCC (2 x 2min). The tissue was dehydrated through a series of ethanol solutions, from 50% to 100% (3min each). The slides were vacuum dried for 30min and stored dessicated at -80°C until used.

3.11.2 Template generation and *in vitro* transcription

In each case, the DNA fragments specific for the mRNA of interest were generated by PCR and cloned into the pAL vector. The sequence of the probe and integrity of the T3 and T7 promoters were verified by sequencing (3.8).

A murine specific riboprobe corresponding to nucleotides 6231-6584 of $Ca_v3.1$ was generated. The DNA template was amplified from the murine cDNA clone using primers EM4 and LVA4, which are specific for the variable carboxy terminal region of the protein. The template was blunt-end ligated into vector pAL (3.5.4).

The murine γ2 and γ4 specific riboprobes were generated by amplifying highly variable regions of the template from murine clones using forward and reverse primers to which *Bam*H1 and *Asp*718 restriction sites had been added, respectively. This approach allowed for sticky-end cloning and the correct orientation of the insert in the vector. Primers G2F and G2R were used to amplify nucleotides 820-947 of γ2, and primers G3F and G3R for nucleotides 839-980 of γ4 (7.3).

For both $\alpha_2\delta-1$ and $\alpha_2\delta-3$ the probes were selected to be in the variable C-terminal region of α_2 in order to avoid cross-reactivity between isoforms. *Bam*H1 and *Asp*718 restriction sites were added to the $\alpha_2\delta-1$ forward and reverse primers (EM10 and EM11), respectively, to allow for sticky-end ligation to vector pAL. Primers AD13 and AD15 were used to amplify $\alpha_2\delta-3$ from the cloned murine cDNA. The template for $\alpha_2\delta-3$ was blunt-end ligated into the pAL vector.

RNA grade reagents and water were used for the transcription and hybridisation procedures. Sense and anti-sense probes were generated from the template, with the T3 promoter used for the transcription of the sense, and the T7 promoter for the anti-sense probes. For each probe approximately 12µg of template cDNA in the pAL plasmid was linearised using *Bam*H1 and, separately, *Asp*718. The enzymes were removed by phenol-chloroform extraction and the DNA precipitated. A 20µl transcription reaction was set up, consisting of: 1µg linearised cDNA template, 1 x transcription buffer, 37.5M DTT, 0.5M each rATP, rGTP and rCTP, 48U RNasin, 75µCi ^{35}S-UTP and 25U T3 or T7 polymerase (T3 polymerase was used when the DNA was linearised with *Asp*718, T7 polymerase when linearised with *Bam*HI). The reaction was allowed to proceed for 30min at 37°C, an additional 25U T7 or T3 polymerase was added, and incubated for a further 40min. Template DNA was digested with DNase 1 (27U) for 10min at 37°C. The volume was made up to 50µl with TE buffer and the radioactively labelled probe separated from unincorporated nucleotide using a Sephadex G-50 Nick-column (3.9.2). Probe activity was measured by scintillation counting (5µl of probe in 1ml scintillant) and diluted to $1x10^7$dpm/ml in hybridisation buffer (10mM Tris pH 8.0, 0.3M NaCl, 1mM EDTA, 1 x Denhardts, 10% dextran, 50% deionized formamide, 50mM DTT and 0.5µg/µl tRNA). Prior to performing the reaction with radioactive nucleotide, the templates and enzymes were tested in a 'cold' assay using unlabelled rUTP, and the successful generation of transcripts assessed by electrophoresis of the products in a 2% agarose gel. Once it was established that the promoters were functional and that the products were of the correct size, transcription was performed using ^{35}S-rUTP.

3.11.3 *In situ* hybridisation and autoradiography

Hybridisation with radiolabelled probe (approximately 60µl per section) proceeded for 16hrs at 55°C in a humidified container. The sections were washed in 2 x SSC, 1mM EDTA, 1mM DTT and

treated with 20µg/µl RNase in 0.2M Tris pH 8.0, 1M NaCl and 0.1M EDTA to remove unbound probe. A high stringency wash of 0.1 x SSC, 1mM EDTA, 1mM DTT was done for 2hrs at 60°C. The slides were dehydrated in a 50-100% ethanol series (3min each) and analysed by autoradiography. Following autoradiography, the slides were coated with NTB-2 liquid film emulsion and developed after 3-4 weeks. The slides were counterstained by immersion in 1% toluidine blue (1-5min), rinsing in water and destaining in 70% ethanol until the desired colour intensity was obtained. The slides were dehydrated in xylol and coverslipped using DEPEX. The sections were examined under dark- and bright-field illumination.

3.12 Expression of proteins in eukaryotic cells

Since the expression of calcium channel subunits overlaps in many tissues, it was necessary to express the proteins of interest in mammalian cell lines to distinguish between the various family members.

3.12.1 Culture of HEK293 and COS-7 cells

Human embryonic kidney cells (HEK293) were maintained at 37ºC, 5%CO_2 in minimal essential medium (MEM) with 1.8mM L-glutamine, 0.2% $NaHCO_3$, 10% foetal calf serum (FCS), 100U penicillin and 100µg/ml streptomycin. The cells were passaged when they approached confluency by trypsinising with 0.05% trypsin/0.2% EDTA and seeding into fresh medium. African green monkey kidney cells (COS-7) were maintained in Dulbecco's MEM (DMEM) containing 10% FCS, 100U penicillin and 100µg/ml streptomycin at 37°C, 5% CO_2. The cells were similarly passaged. Aliquots of cells were periodically frozen away in medium containing FCS + 10% DMSO. HEK293 cells were used for lower levels of protein expression and for electrophysiological measurements, while COS-7 cells were used for larger scale production of protein.

3.12.2 Calcium phosphate transfection of HEK293 cells

Plasmids containing the calcium channel subunits were transiently transfected in human kidney embryonic cells (HEK293) using the calcium phosphate method. Cells were seeded on day 1 in 10 x 100mm culture plates at $1x10^6$/plate and grown overnight. Transfection was performed late on day 2. The 10ml transfection mixture consisted of 15µg total plasmid DNA 500µl 2.5M $CaCl_2$

added dropwise, and 5ml 2 x BBS, pH6.95. 1ml of the transfection solution was added to each plate. The plates were incubated overnight in a humidified incubator at 35ºC, 3%CO_2. The cells were washed early on day 3 with 1 x PBS until the calcium phosphate precipitate was removed. Following 24hrs incubation at 37ºC, 5%CO_2, the cells were loosened from the plates using a cell scraper, collected, washed with PBS, and the cell pellet frozen at -80ºC until processed.

3.12.3 FuGene transfection of COS-7 cells

In order to obtain a higher transfection efficiency, the transfection reagent FuGene 6 was used. Plasmids containing the $\alpha_2\delta$ subunits, or pcDNA3 as control, were transiently transfected in COS-7 cells using FuGene 6. The COS-7 cells were seeded at $1.5x10^6$ cells per 100mm culture plate. After 24hrs the cells were transfected in antibiotic-free medium with 6µg DNA using 18µl of FuGene reagent per plate. The medium was replaced with complete medium after 16hrs and harvested 60-72hrs after the start of transfection.

3.12.4 a$_2$d-Myc-His tag constructs

With a view to purify the $\alpha_2\delta$ subunits and obtain sequence information of the post-translational cleavage sites, a Myc-His tag was added to the carboxy terminal ends of the $\alpha_2\delta$–2 and -3 proteins. This was achieved by sub-cloning the $\alpha_2\delta$ sequences (with stop codon removed) into the pcDNA3.1/Myc-His vector. A PCR approach was used to amplify sequences corresponding to the carboxy terminal of the clones using primers that lacked the stop codon. The constructs were sequenced to ensure that the stop codon had been removed, and that the Myc-His tag was in-frame with the $\alpha_2\delta$ reading frame. The procedure is described in more detail below.

For $\alpha_2\delta$–2, a unique *Nhe*I site situated in the putative δ sequence was used together with the 3' multiple cloning *Xho*I site to excise a section of the DNA containing the stop codon. The forward primer ad2His1 (with *Nhe*I site) and reverse primer ad2His2 (with the modified sequence without stop codon and a *Xho*I site) were used to amplify the replacement 3' end sequence. The restricted PCR product was then ligated to the remaining $\alpha_2\delta$-2 sequence. This was subcloned into pcDNA3.1/Myc-His using the *Acc*65I site in the upstream multiple cloning site, and the 3' *Xho*I site.

A single-cutting *Bfr*I site in $\alpha_2\delta$−3 was similarly used together with the multiple cloning *Apa* I site to remove the sequence containing the stop codon. The forward primer a2d3His1, with a *Bfr*I site, and the reverse primer a2d3His2 with an *Apa*I site for ligation with the remaining $\alpha_2\delta$−3 sequence was used to amplify the modified sequence. A *Xba*I site was added to the a2d3His2 primer to allow for easier insertion into the pcDNA3.1/Myc-His vector. As with $\alpha_2\delta$−2, this modified sequence was restricted, used to replace the end of $\alpha_2\delta$−3, and subcloned into pcDNA3.1/Myc-His.

The $\alpha_2\delta$ (- stop + tag) proteins were subsequently expressed in eukaryotic cells (3.12.2 and 3.12.3) and analysed by immunoblotting (3.15.2).

3.13 Protein techniques

3.13.1 Microsomal membrane preparations

Tissues from Balb/c mice were crushed under liquid nitrogen using a mortar and pestle. The powder was homogenized in Buffer A (20mM MOPS, pH 7.4, 300mM sucrose, 2mM EDTA, 1mM iodoacetamide, 1mM orthophenanthroline, 0.2mM phenylmethylsulfonyl fluoride, 1mM benzamidine, 1µg/ml leupeptin, 1µg/ml pepstatin A and 1µg/ml antipain) by two 20s bursts with a Polytron and 8 strokes in a Potter. Cell debris was pelleted by centrifugation at 5000g for 10min at 4°C. Low speed pellets were re-extracted as above and the supernatants combined. The supernatants were centrifuged at 70 000g for 30min at 4°C. The pellets were resuspended in Buffer A and stored in aliquots at -80°C. Membranes from transfected COS-7 cells were prepared similarly, with the following modifications: cells were harvested by scraping into 1 x PBS, pelleted by low speed centrifugation, resuspended in 5mM Tris-Cl, 5mM EDTA, pH 7.4 containing protease inhibitors (as above) and incubated on ice for 15min prior to homogenisation. The pellets resulting from ultracentrifugation were resuspended in 50mM MOPS pH 7.4 plus protease inhibitors. The protein content was determined by the Bradford method using BSA as a standard (3.13.2).

3.13.2 Determination of protein content

The protein content of membrane preparations was estimated using the Bradford protein determination method. Bovine serum albumin (BSA) standards were prepared from concentrations of 25 to 100ng/µl in water. 1ml of Bradford solution was added to 100µl of standard or diluted

sample, left at room temperature for 5min, and the absorbance measured at 595nm. A calibration curve of the protein concentration versus absorbance was constructed and the sample concentration calculated.

3.14 Anti-peptide antibodies

Polyclonal antibodies were raised in rabbits by Gramsch Laboratories (Schwabhausen, Germany) against peptides of the human $\alpha_2\delta$–2 (a.a. 98-115) and murine $\alpha_2\delta$–3 (a.a. 59-76) subunits. These sequences were selected as they have low homology to each other and to $\alpha_2\delta$-1, are found after the putative signal peptide sequence, and have no potential N-glycosylation sites.

$\alpha_2\delta$-2: NH_3- **YKDNRNLFEVQENEPQKL*WC*** - COOH

$\alpha_2\delta$-3: NH_3- **KYSGSQLLQKKYKEYEKD*WC*** - COOH

A tryptophan (W) residue was added to the carboxy terminal of each peptide to allow for spectrophotometric detection. The cysteines (C) permitted coupling of the peptides to the adjuvant as well as coupling to columns for antibody purification.

3.14.1 Purification of antibodies using immunoaffinity columns

The polyclonal antibodies were separated from the rest of the serum proteins by immunoaffinity chromatography. The antigen peptides were bound to sulfhydryl linkers of a Sulfolink resin via the carboxy terminal cysteines. In order to ensure a high efficiency of binding of peptide to column, the peptides were reduced using dithiotreitol (DTT). 10mg of peptide was added to a 750µl solution of degassed TE, pH 8.5, containing 0.1M DTT and incubated for 1hr at room temperature. The peptide was separated from DTT using a G-10 Sephadex column equilibrated in TE. 1ml fractions were collected and 50µl fractions set aside for monitoring the absorbance of the aromatic amino acid tryptophan at 280nm. Fractions containing the peptide were combined. A 2ml packed volume of Sulfolink gel was equilibrated in TE for 15min at room temperature. Following a brief centrifugation to settle the gel, it was resuspended in fresh TE. The fractions containing the reduced peptide were added to the gel on ice and the volume made up to 4ml. After mixing and a brief centrifugation, a 50µl aliquout was removed and used to estimate the total amount of peptide available for binding (pre-coupling value). The gel and peptide were rotated slowly at room temperature for 2hrs. Before a wash with TE, a 50µl aliquot of supernatant was removed to estimate the total amount of peptide

not bound to the gel (post-coupling value). The efficiency of the peptide coupling could be calculated as a percentage of the bound peptide (post-coupling) relative to the peptide available for binding (pre-coupling).

In order to block sulfhydryl sites not bound to the peptide and to prevent non-specific binding of antibody to the column at a later stage, the Sulfolink gel was incubated with 50mM cysteine in TE for 1hr at room temperature. The cysteine solution was removed and the gel resuspended in 1M NaCl. A 10cm, 4ml column was packed with the gel and washed with 65ml NaCl, using a peristaltic pump. The column was equilibrated with 50ml of PBS, pH 7.4. Two ml of serum was diluted 6x with PBS and filtered through a 0.2µm filter. The serum was circulated slowly over the column overnight at 4ºC.

Prior to elution, the column was washed with 150ml PBS, 0.5M NaCl, followed by 100ml PBS, 0.5M NaCl, 0.1% Tween-20 and finally by 50ml PBS. The antibodies were eluted with 4.5M $MgCl_2$, and 1ml fractions collected in an equal volume of PBS in YM-50 centrifugal filter devices designed to retain molecules larger than 50 000Da. The salt was reduced by centrifuging 3 times (5 000g, 30min, 4ºC) to dead stop volume and increasing the volume to 2ml with PBS. The antibody was made to 1mg/ml BSA in PBS and stored at -20°C in aliquots.

3.15 Analysis of membrane proteins by Western/Immunoblotting

3.15.1 SDS-PAGE and electroblotting

Proteins were separated by discontinuous SDS-PAGE (SDS polyacrylamide gel electrophoresis). Resolving gels of 5 or 7.5% (in 0.375M Tris-Cl pH 8.8, 0.1% SDS) were prepared, with a 3% stacking gel (in 0.125M Tris-Cl pH 6.8, 0.1% SDS). The membrane preparations were denatured in Laemmli sample buffer (0.25M Tris-Cl pH 6.8, 1.6% SDS, 5% glycerol, bromophenol blue, with or without 0.1M DTT) by boiling for 3min. Typically, 50-100µg of tissue protein or 3µg of cultured cell protein was loaded per lane. The gels were run at 100V in 25mM Tris, 0.2M glycine, 1%SDS. The gel and Hybond ECL nitrocellose membrane were equilibrated for 15min in transfer buffer (25mM Tris, 192mM glycine, 20% methanol, pH8.3) before electroblotting. Transfer conditions were 300mA for 1hr, using a ice block to cool the system.

3.15.2 Western/Immunoblotting

Nitrocellulose membranes were blocked 16-64hrs in 3% BSA in TBST (1 x TBS, 0.1% Tween-20). Following a wash in TBST for 15min, the membranes were incubated at room temperature for 2hrs in primary antibody solution in TBST containing 1µg/ml BSA. The antibody dilutions were 1/500 for $\alpha_2\delta$–1 and -3, and 1/750 for $\alpha_2\delta$–2. The blots were washed three times for 10min in TBST. Incubation with the secondary antibodies, goat anti-rabbit- or goat anti-mouse-horseradish peroxidase, proceeded for 1hr at room temperature at a dilution of 1/7 000 in TBST. Following washing as above, antibody binding was detected using an enhanced chemiluminescence (ECL) system. Equal volumes of solutions 1 and 2 were combined and the membrane incubated in the mixture at room temperature for 1min. The membrane was briefly blotted to remove excess liquid and exposed to ECL Hyperfilm for 10-120s. The films were developed using an automated developing machine.

3.16 Immunocytochemistry

To test whether the constructs expressing $\alpha_2\delta$ proteins were functional, polyclonal antibodies were applied to fixed cells and detected using fluorescent secondary antibodies.

HEK293 cells were seeded at 30 000/well onto polylysine-coated cover slips in a 24 well plate. The cells were transfected after 16hrs using the $CaPO_4$ protocol (3.12.2). 25µg of DNA per well was used for the overnight transfection. The cells were washed in PBS and grown for 2 days. Following a PBS wash, the cells were fixed with 2% paraformaldehyde in PBS for 20min at room temperature. After two PBST (PBS + 0.1% Tween-20) washes, the cells were blocked with 5% normal goat serum in PBST for 30min. The primary antibodies were applied at a concentration of 1/500 in blocking solution for 2hrs at room temperature. After 3 washes with PBST, CY-3 conjugated goat anti-rabbit IgG was applied for 1hr in the dark. The excess antibody was removed by two washes with PBST and a final PBS wash. The cover slips were mounted onto slides with 90% glycerol and the edges sealed with clear nail polish. The fluorescent CY-3 was excited at 546nm and the cells photographed

3.17 Deglycosylation assay

70µg of membrane protein was denatured by boiling in 0.1M β-mercaptoethanol, 0.5% SDS for 5min. The reaction mixture was brought to 15mM Tris pH 8.0, 20mM orthophenanthroline and 1% Triton-X 100. Two units of N-glycosidase F were added and the reaction allowed to proceed for 5hrs at 37°C. The protein was analysed by immunoblotting (3.15.2).

3.18 Gabapentin binding assay

10 to 30µg of COS-7 membrane preparations were incubated in 200µl volumes with various concentrations of [^{3}H]-gabapentin (143Ci/mmol) in 10mM Hepes/KOH, pH 7.4, for 30min at room temperature. The protein was precipitated using 8ml of ice-cold precipitation buffer (22.5mM Hepes, pH 7.4; 11,25% PEG 6000; 11,25mM $CaCl_2$) and filtered over GF/B filters soaked in the same buffer. Two further 8ml volumes of precipitation buffer were used as washes. The activity of the filters were counted in a scintillation counter. Concentrations greater than 20nM were achieved by adding non-radioactive gabapentin to the required concentration. The corrected binding was calculated using:

$$\text{Total GBP bound} = (\text{specific dpm}) \times \left(1 + \left(\frac{\text{concentration non-radioactive gabapentin}}{\text{concentration } [^3\text{H}] - \text{gabapentin}}\right)\right).$$

Non-specific binding was determined in the presence of 10µM of unlabelled gabapentin. The background binding was less than 20% of the counts without unlabelled gabapentin.

To determine the K_d (protein-ligand affinity constant or dissociation constant), the equilibrium binding of the ligand (GBP), to the protein was studied as a function of ligand concentration at a fixed protein concentration (COS-7 membrane preparation). The Scatchard plot is one way of determining the K_d of an interaction. The Scatchard equation is:

$$\frac{B}{F} = -\frac{1}{K_d}B + \frac{T}{K_d}$$

Where *B* is the number of moles of ligand *B*ound to each mole of protein, K_d is the affinity constant, *F* is the molar concentration of *F*ree (unbound) ligand and *T* is the *T*otal amount of protein. It is possible to determine the value of K_d by plotting *B*/*F* vs. *B*. The plot is biphasic if the binding is co-operative, or if there are more than one set of binding sites which have different affinities.

3.19 Electrophysiological analyses

The full length cDNA's of the subunits cloned in pcDNA3 were transiently transfected in HEK293 cells. The subunits were transfected with the DNA at a ratio of 1:1 using Lipofectamine. The petri dishes with transfected cells were mounted on an inverted microscope and constantly perfused with Tyrode's solution. Ionic currents were recorded by means of a whole-cell patch clamp. In the following description, the extracellular solution for LVA channels is shown in brackets when it differs from that used for HVA channels. The bath solution typically contained 125mM *N*-methyl-D-glucamine, 5mM CsCl, 1mM $MgCl_2$, 10mM HEPES and 5mM glucose (10mM), and was set to a pH of 7.4 using HCl. 10 or 20mM of Ba^{2+} ($BaCl_2$) or Ca^{2+} ($CaCl_2$) were included in the solutions as charge carriers. The pH was set to 7.4 using HCl. The pipette solution for HVA and LVA channels contained 60mM CsCl, 1mM $CaCl_2$, 1mM $MgCl_2$, 5mM K_2ATP, 10mM HEPES, 50mM aspartic acid and 10mM EGTA. The pH was adjusted to 7.4 using CsOH. When Ba^{2+} current was measured, 0.1mM EGTA was included in the bath solutions.

Currents were recorded using an EPC-9 patch clamp amplifier and Pulse software from Heka Electronics (Lambrecht, Germany). Patch pipettes were pulled from borosilicate glass. The pipette input resistance was usually between 1.8 and 2.0MΩ. The capacitance of individual cells ranged between 15 and 90pF, and series resistance ranged between 3.5 and 5.0MΩ. Capacitance transients were compensated using built-in procedures of the Heka system. Curve fitting and statistical analysis were performed with Origin 6.0 (Microcal, USA). The statististical significance was evaluated by nonpaired Student's *t* test. A $p<5\%$ was considered to be significant.

To demonstrate the voltage protocols used and the data evaluation, representative traces, plots and schematic representations are shown in Figure 4. To determine the current-voltage (I-V) relationships, currents were activated by 40ms long depolarizations from the holding potential, in 10mV steps, to 10 or 20mV above the reversal potential (Figure 4A and B). The current density was calculated and expressed as pA/pF. The half-maximal voltage of activation can be calculated by normalizing the individual inward current peaks to the maximum current, and fitting the ascending part of the I-V curve to the Boltzmann equation. The $V_{0.5act}$ is the voltage at which half the channels are activated, and the kinetics of activation determined from the slope (Figure 4B). To calculate the half-maximal inactivation potential ($V_{0.5inact}$) a steady-state inactivation protocol was used (Figure 4C).

The channels were inactivated by a 5s long prepulse in a step-wise fashion to various depolarizing potentials. Following a prepulse, the current amplitude was measured during a 40ms test pulse to the voltage at the peak of the I-V curve. The time constant of activation was calculated from monoexponential fits of the I-V traces (Figure 4D). The time constants of inactivation were calculated from bi-exponential fits of traces activated by 5s long pulses to the peak of the I-V (E).

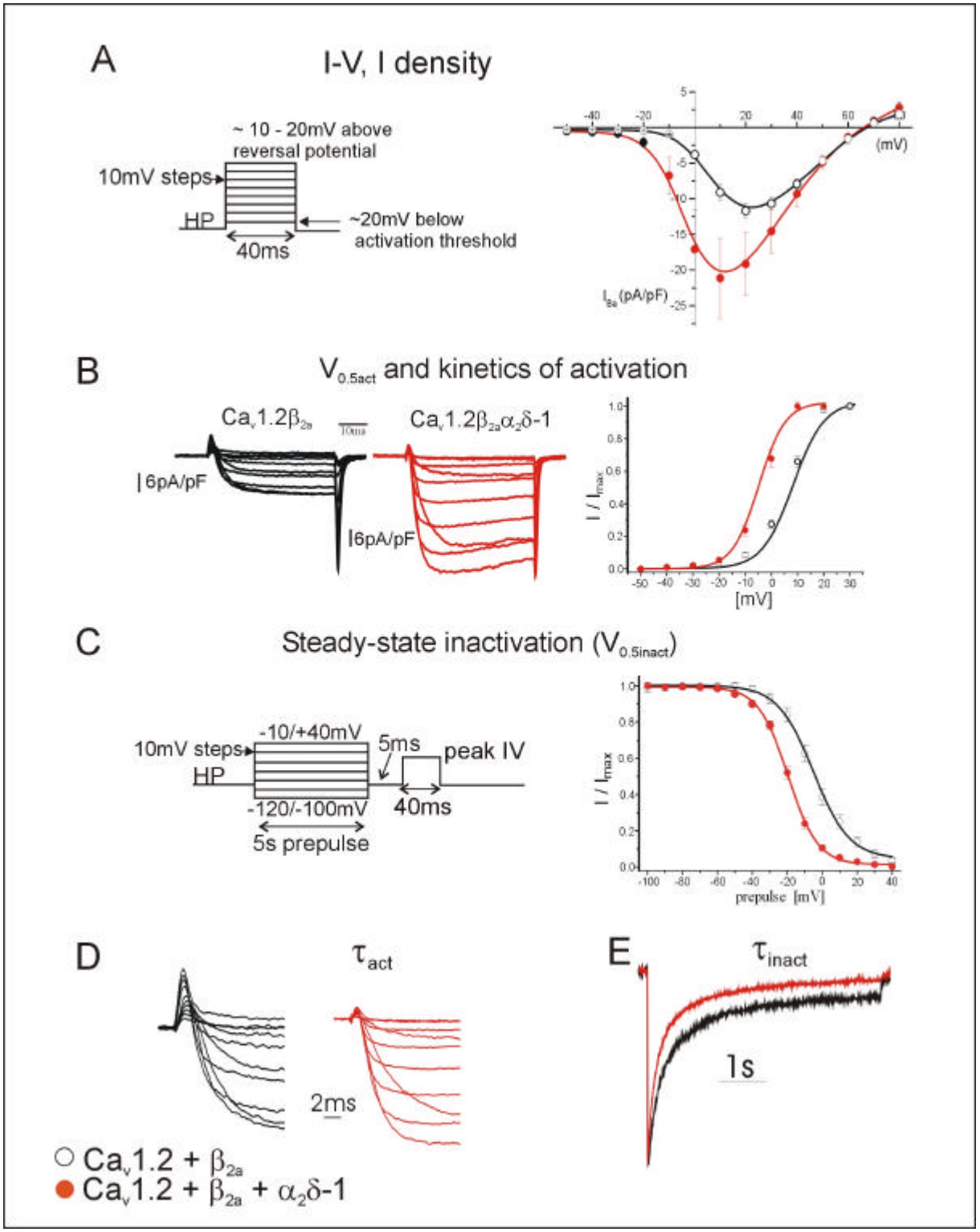

Figure 4: Typical voltage protocols and analyses used for functional characterisation of the calcium channel subunits. Data from the $Ca_v1.2$ + β_{2a} channel without (○) and with (●) $\alpha_2\delta$-1 are shown as an

example. In (A), the protocol used to obtain a **I-V** (current-voltage) relationship is indicated. The half-maximal voltage of activation ($\mathbf{V_{0.5act}}$) and kinetics of activation were calculated by fitting the Boltzmann equation to the ascending part of the I-V data (B). The steady state inactivation ($\mathbf{V_{0.5inact}}$) was measured using the voltage protocol shown in C. The voltages used depended on the type of channel expressed. The traces used for calculating the time constants (t) of activation and inactivation are shown in (D) and (E). **HP** is the holding potential.

3.20 Solutions and media

All solutions were autoclaved unless otherwise specified.

2 x BBS: 50mM BES, 280mM NaCl, 1.5mM Na_2HPO_4, pH 6.95. Stored at -20°C.

Bradford reagent: 100mg of Coomassie Brilliant Blue G250 was dissolved in 50ml 95% ethanol. 100ml of 95% phosphoric acid was added, the solution was made to 1l with distilled water and filtered.

50 x Denhardts: 1% Ficoll, 1% polyvinylpyrolidine, 1% BSA. The solution was filter sterilised and stored at -20°C.

LB (+) medium: 10% SELECT Tryptone, 5% Yeast extract, 5% NaCl, 1% D(+) glucose. The medium was autoclaved and the required selection antibiotics added when the solution had cooled to 55ºC.

1 x PBS : 0.17M NaCl, 2.7mM KCl, 8mM Na_2HPO_4, 1.7mM KH_2PO_4, pH 7.4.

1 x PE: A solution consisting of 0.5% sodium pyrophosphate, 5% SDS, 1% polyvinylpyrolidine, 1% Ficoll 400 000, 0.25M Tris-Cl pH 7.5, 25mM EDTA pH 8.0 was prepared and dissolved at 65°C. BSA to 1% was added when the liquid had cooled to 37°C. The solution was filter sterilised and stored at -20°C.

1 x SSC: 0.15M NaCl, 15mM sodium citrate.

1 x TBE: 90mM Tris, 90mM boric acid, 2mM EDTA pH 8.0.

1 x TE : 10mM Tris-Cl, 1mM EDTA, pH 8.0

4 Results

One of the main thrusts of this project was to identify physiological interactions between the novel voltage gated calcium channel subunits cloned in our laboratory ($Ca_v3.1$, $\alpha_2\delta$-2 and -3, γ3, γ4 and γ5). This was achieved by determining the mRNA distribution of the subunits in several tissues, followed by a detailed study of neuronally expressed subunits in mouse brain by *in situ* hybridisation. It was then assessed whether the subunits interact functionally in a mammalian expression system, as judged by the electrophysiological characteristics of the channel current. Based on these results, an interaction profile could be inferred. A second goal was to characterise the novel $\alpha_2\delta$-2 and -3 subunit proteins in terms of structure and drug binding properties. The results of these analyses are presented below.

4.1 Distribution of $Ca_v3.1$ (α_{1G}) mRNA in brain

Although most HVA channels were cloned several years ago, the genes for LVA channels remained elusive until recently. It was only through a change in the strategies used for database searches, and by application of *C.elegans* cDNA information for library screens, that the T-type channels could be cloned. In our laboratory $Ca_v3.1$ was cloned from mouse brain using a probe based on a *C.elegans* sequence (Klugbauer et al. 1999b). Northern analysis had shown a strong expression of $Ca_v3.1$ in mouse brain with a weaker signal in heart. In order to map the expression of $Ca_v3.1$ in mouse brain, *in situ* hybridisation with a $Ca_v3.1$ specific probe was performed.

The thalamus, olfactory bulb and cerebellum showed high expression of the transcript, with moderate expression in the hippocampus and cerebral cortex (Figure 5). Examination of slides coated with photographic emulsion revealed that expression was strongest in the Purkinje cell layer in the cerebellum, and in the granular, mitral and glomerular layers of the olfactory bulb. In the hippocampus, $Ca_v3.1$ expression predominated in the granular cell layer of the dentate gyrus and pyramidal neurons of CA1-3. Hybridisation with the sense probe showed that the hybridisation was specific (Figure 9A)

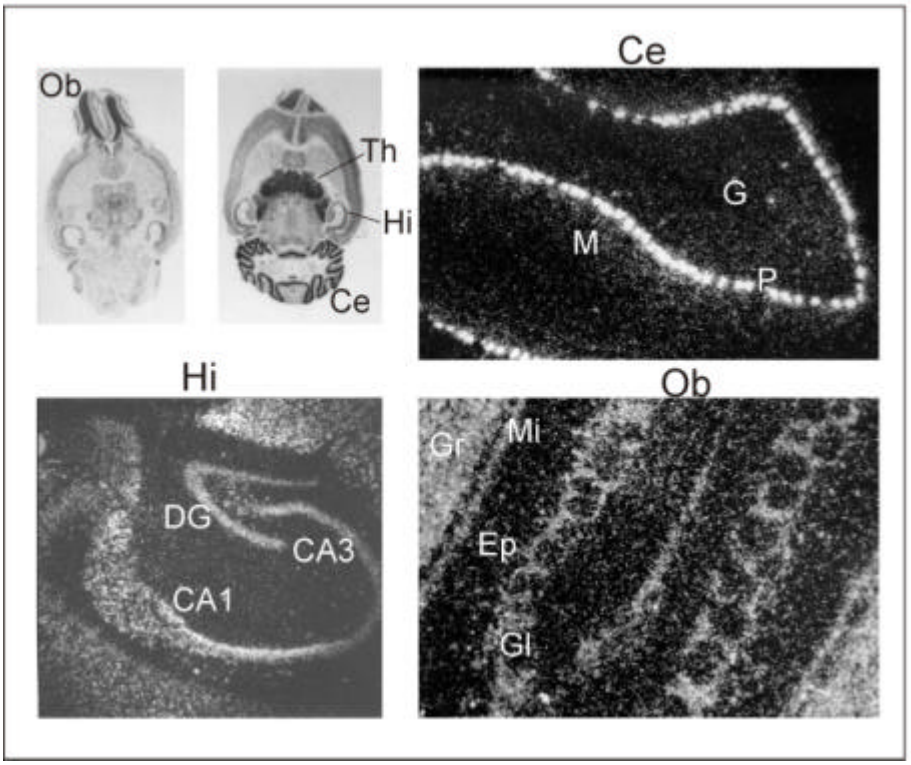

Figure 5: The $Ca_v3.1$ (α_{1G}) T-type channel is expressed in a region-specific manner in mouse brain. Autoradiographs of *in situ* hybridisation of basal and central horizontal sections of the brain are shown. Dark-field views of photographic emulsion coated slides show expression in cerebellum (**Ce**), olfactory bulb (**Ob**) and hippocampus **(Hi**). The labels indicate the molecular layer (**M**), granular layer (**G**) and Purkinje cell layer (**P**) in the cerebellum, the dentate gyrus (**DG**), the **CA1** and **CA3** regions of Ammon's horn in hippocampus, and the mitral (**Mi**), glomerular (**Gl**), granular (**Gr**) and external plexiform (**Ep**) layers in the olfactory bulb. Original magnifications are 100x for the Ce and Ob, and 50x for the Hi.

4.2 γ subunits in brain

A comparison of mRNA expression patterns of the neuronal γ subunits (γ2, γ3 and γ4) in mouse was performed by *in situ* hybridisation. The distribution of these subunits differed considerably. γ2 was strongly expressed in the cerebellum and hippocampus, with intermediate levels in the cerebral cortex and olfactory bulb (Figure 6A). γ3 was detected in the hippocampus and cerebral cortex with lower levels seen in the olfactory bulb and caudate putamen[1] (Figure 6C). In contrast to γ2 and γ3, γ4 was highly expressed in the caudate putamen, olfactory bulb and habenulae, with weaker signals in the cerebellum and thalamic nuclei (Figure 6B). The specificity of the hybridisations was assesed using sense probes (Figure 9B).

[1] γ3 ISH done by G. Bohn. The probe corresponds to nucleotides 748-912 of murine γ3.

To identify the cell layers containing the transcripts, emulsion coated slides were examined under higher magnification. γ2 was found in the CA1-CA3 and granular cell layers of the dentate gyrus (hippocampus) as well as the Purkinje cell layer of the cerebellum (Figure 6A). γ4 mRNA localised to the the glomerular, mitral and granular cell layers of the olfactory bulb and the cerebellar Purkinje cell layer (Figure 6B). While γ2 appears to be localised to the Purkinje cell bodies, the γ4 signals could originate from processes of the Purkinje cells or associated basket cells.

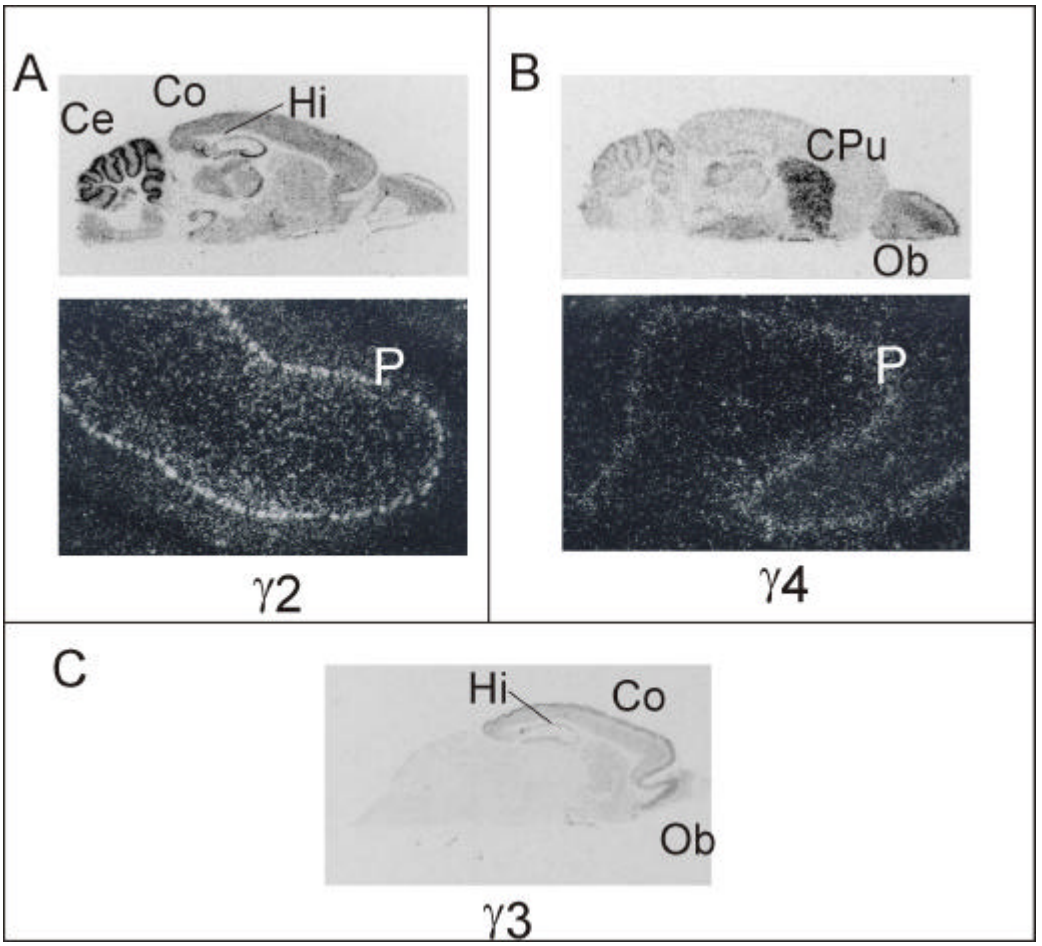

Figure 6: The neuronal γ subunits are differentially distributed in mouse brain. Autoradiographs of hybridisations done *in situ* on sagittal sections of brain are presented. γ2 is broadly expressed (A), with strong signals seen in the cerebellum (**Ce**), hippocampus (**Hi**) and cortex (**Co**). γ3 is only moderately expressed in the cortex and olfactory bulb (**Ob**) (C), whereas γ4 has a clear localisation in the caudate putamen (**Cpu**) and olfactory bulb (B). The dark field views below γ2 and γ4 show the cerebellum, with expression in the Purkinje cell layer (**P**).

4.3 Distribution of $\alpha_2\delta$ mRNA

The tissue distribution of $\alpha_2\delta$-1 and the novel $\alpha_2\delta$-2 and –3 subunits was first established by dot or Northern blotting using isoform specific probes. Their expression in mouse brain was then studied in detail by *in situ* hybridisation.

4.3.1 Northern analyses

The expression of $\alpha_2\delta$ subunit mRNA in tissues was assessed by Northern blotting. Hybridisation of a human mRNA dot blot with a specific probe showed that $\alpha_2\delta-1$ is ubiquitously expressed, with the strongest signals seen in skeletal muscle, pituitary gland, kidney, lung, small intestine as well as foetal brain and kidney (Figure 7A). A predominant 5.2kb $\alpha_2\delta-2$ transcript was observed at high levels in human heart, pancreas and skeletal muscle, with weaker signals in brain, liver and kidney[2] (Figure 7B). Signals were detected in all tissues when the blot was exposed for a longer period. This pattern was also seen in a mouse multiple tissue Northern blot (not shown). In contrast to the $\alpha_2\delta-1$ and -2 subunits, $\alpha_2\delta-3$ is a solely neuronal form, with a hybridisation signal seen at 4.3kb in brain (Figure 7C).

[2] $\alpha_2\delta$-2 Nothern blot done in cooperation with M.Hobom

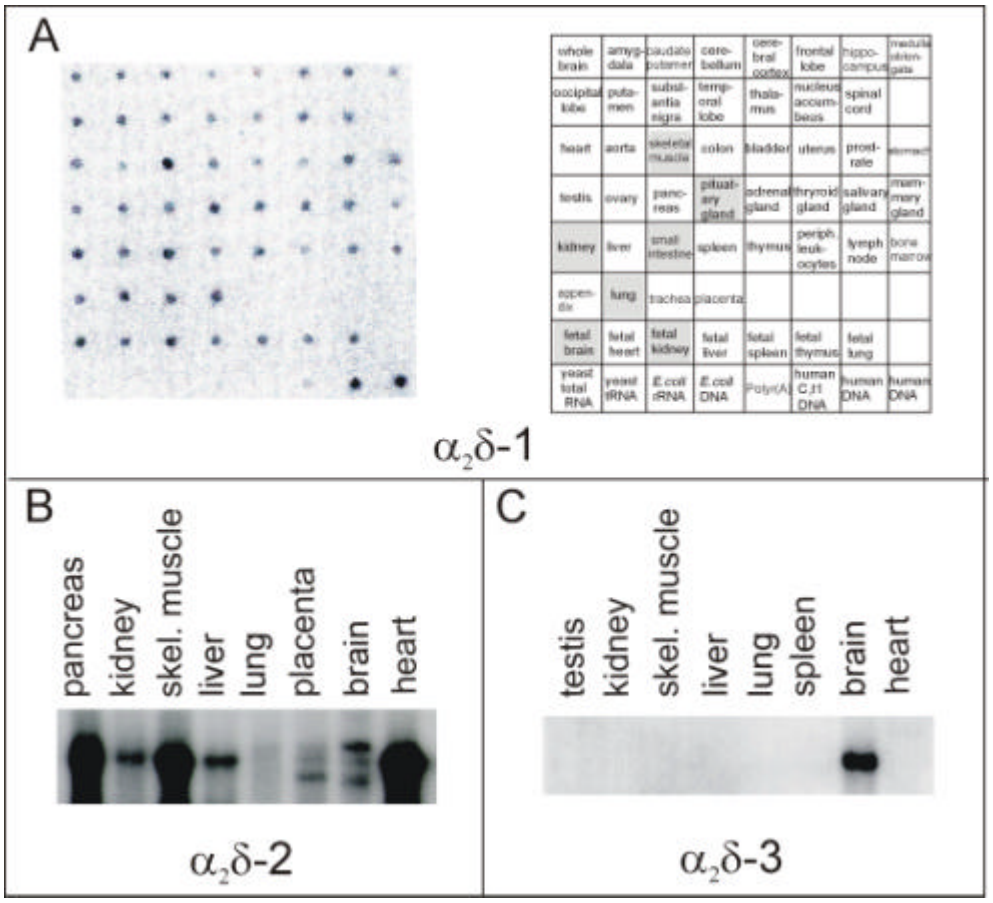

Figure 7: Dot blot and Northern blot analysis of the tissue distribution of $\alpha_2\delta$-1, -2 and -3. A human dot blot was probed with an $\alpha_2\delta$-1 specific probe (A). A positional grid is shown for identification of the tissues. No signal was seen for yeast, *E.coli* or C_0t repetitive sequences. Labels on a grey background indicate the tissues with the highest expression levels. A human Northern blot probed with an $\alpha_2\delta$-2 probe (B) and a murine blot for $\alpha_2\delta$-3 (C) are also shown.

4.3.2 Localisation of a 2d subunits in brain by *in situ* hybridisation

Since all three subunits were found to be expressed in mouse brain, a more detailed mapping of $\alpha_2\delta-1$, -2 and -3 mRNA distribution was performed by *in situ* hybridisation. $\alpha_2\delta$ transcripts were detected in several regions of the brain, with a distinct pattern for each subunit. Hybridisation of the anti-sense probes were judged as specific, as hybridisation with the sense sequences resulted in a negligible background signal (Figure 9C).

A high level of $\alpha_2\delta-1$ mRNA was seen in the pyramidal cell layer of Ammon's horn in the hippocampus (CA1-3) and in the granular cell layer of the dentate gyrus (Figure 8A). The olfactory bulb also hybridised strongly, with signals observed in the mitral and glomerular cell regions. Hybridisation of the probe in the cerebellar cortex, and to a lesser extent in thalamic nuclei, was also observed. Expression of $\alpha_2\delta-1$ in the cerebellum was restricted to the granular layer. $\alpha_2\delta-2$ was

detected in the cerebellum, reticular thalamic nuclei, habenulae and septal nuclei[3] (Figure 8C). The Purkinje cell layer was found to be the source of the cerebellar signal. $\alpha_2\delta$−3 mRNA was predominantly expressed in the caudate putamen, entorhinal complex, hippocampus and cortex (a typical distribution is shown in Figure 8B). As with $\alpha_2\delta$−1, the pyramidal cell layer of the hippocampus (CA1-3) and granular cell layer of the dentate gyrus showed the highest degree of hybridisation with the $\alpha_2\delta$−3 probe.

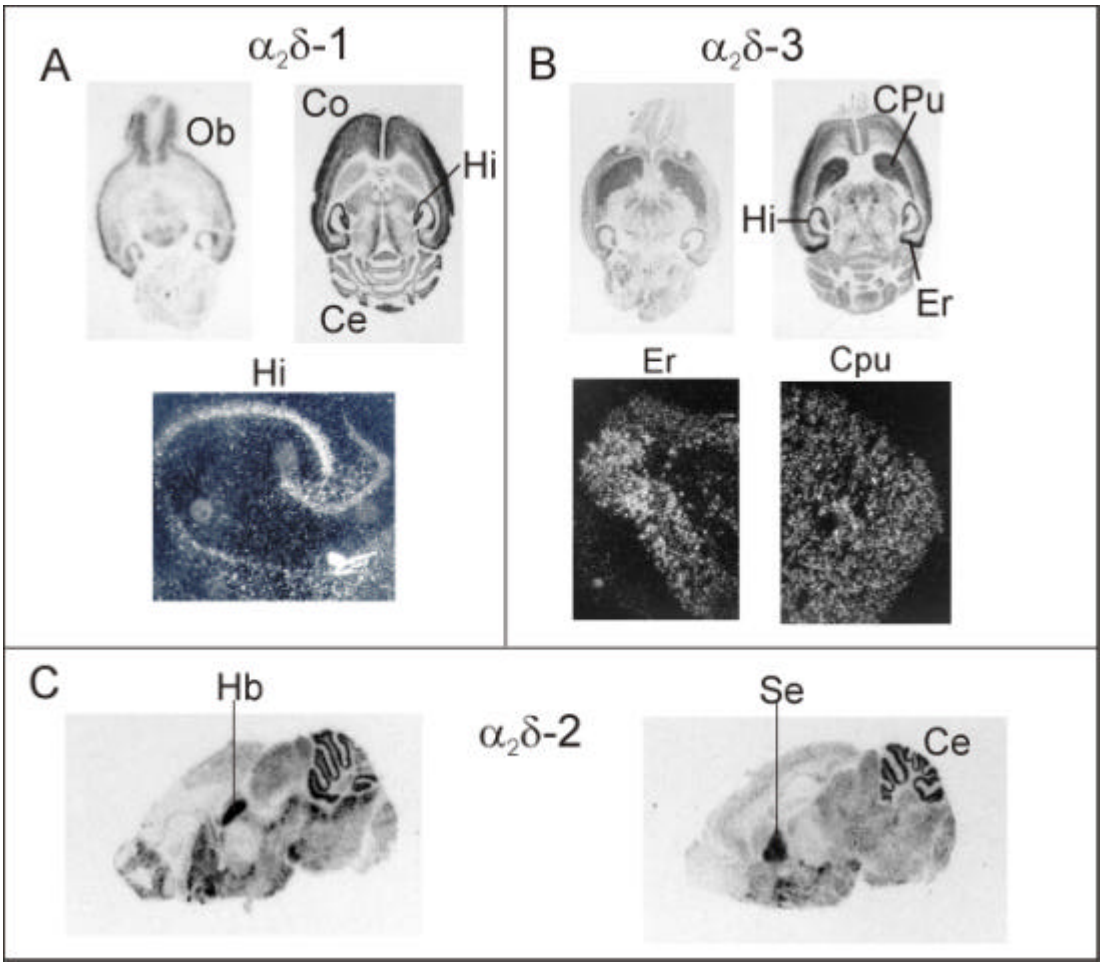

Figure 8: Autoradiographs of $\alpha_2\delta$ subunit expression in mouse brain, as mapped by *in situ* hybridisation. The expression of $\alpha_2\delta$-1 and -3 is shown in basal and central horizontal sections of the brain. $\alpha_2\delta$−1 is prominent in the cerebellum (**Ce**), hippocampus (**Hi**), cortex (**Co**), as well as the olfactory bulb (**Ob**) (A). $\alpha_2\delta$-3 mRNA transcripts were seen in the caudate putamen (**Cpu**), entorhinal complex (**Er**), hippocampus and cortex. Dark field views of $\alpha_2\delta$-3 sections show expression in the **Er** and **CPu**, and in the **Hi** for $\alpha_2\delta$-2 (B). Sagittal sections of brain were used for hybridisation with an $\alpha_2\delta$-2 riboprobe (C), where the strongest signals were seen in the cerebellum, septal nuclei (Se) and habenula (**Hb**).

[3] $\alpha_2\delta$-2 ISH done by M. Hobom. Probes correspond to nt 206-484 and nt 2878-3248

To test whether the anti-sense probes bound specifically to the brain slices, sense probes were generated and hybridised to the tissue under the same conditions. Representative hybridisation of $Ca_v3.1$, $\alpha_2\delta$ and γ sense probes are shown in Figure 9.

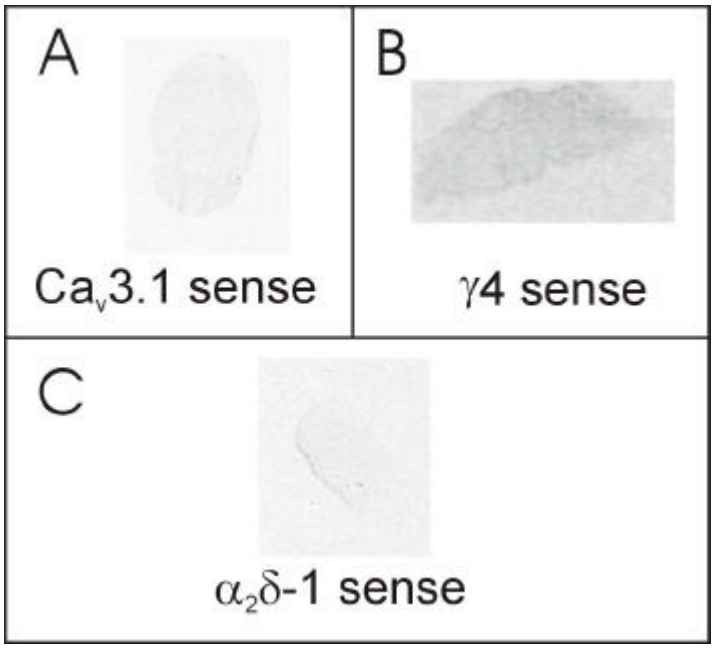

Figure 9: The specificity of the *in situ* hybridisation technique was tested using sense probes transcribed from each construct. Representative hybridisations using sense probes for each subunit type are shown: $Ca_v3.1$ (A), $\gamma4$ (B) and $\alpha_2\delta$-1 (C). In each case the sense hybridisation was negligible.

4.4 Functional characterisation of calcium channel subunits

The novel subunits were expressed together with other subunits in human embryonic kidney cells (HEK293), to form α_1-auxiliary subunit complexes that conduct current. The effects of the auxiliary subunts on current characteristics were then determined by electrophysiological measurements[4]. A significant alteration in the channel properties suggests that the subunits interact *in vivo*.

In this section, the characterisation of a LVA channel, $Ca_v3.1$, is presented, followed by analyses of the auxiliary γ and $\alpha_2\delta$ subunits. In order to gain an overview of the effects of the auxiliary subunits on calcium current, and to extract information on which subunits could interact, summaries of the results are presented below. The numerical data are presented in tabular form in the appendix (7.4).

[4] All electrophysiological experiments were performed by L. Lacinová or S. Dai

4.4.1 Analysis of $Ca_v3.1$ (a_{1G}) current

In order to definitively class the putative mouse $Ca_v3.1$ as a LVA channel, it was necessary to study its electrophysiological characteristics. The cDNA was expressed in HEK293 cells and analysed to determine whether its current characteristics resembled that of native T-type channels and rat $Ca_v3.1$ (Perez-Reyes et al., 1998). For this purpose, Ca^{2+} and Ba^{2+} currents through the channel were measured and compared.

The average current densities did not differ significantly between charge carriers, and were 50.9±7.0 pA/pF (n=23) for Ba^{2+}, and 52.9±8.0 pA/pF (n=15) for Ca^{2+}. Activation of both currents started at -50mV, with the peak current measured at -10mV (Figure 10B). The current traces showed the characteristic cross-over pattern of T-type channels (Figure 10A). Due to kinetic differences the Ba^{2+} and Ca^{2+} traces were not identical. While the activation was similar for both carriers, the Ca^{2+} current inactivated more slowly than the Ba^{2+} current at each membrane potential. The steady state inactivation curves are similar for Ca^{2+} and Ba^{2+}, with half maximal inactivation at -57.3±0.6mV for Ba^{2+} and -55.0±0.5mV for Ca^{2+}. Recovery from inactivation was similarly fast for both ions; 201±12ms for Ba^{2+} and 203±13ms for Ca^{2+}.

T-type current is known to be sensitive to nickel and mibefradil, and the effects of these substances on $Ca_v3.1$ were tested. For nickel, IC_{50} values of 0.47±0.04mM (n=11) for 20mM Ba^{2+} and 1.13±0.06mM (n=11) for 20mM Ca^{2+} (Figure 10C) were calculated. The effects of mibefradil on the channels were tested using Ba^{2+} as charge carrier. $Ca_v3.1$ showed a voltage dependent sensitivity to mibefradil with an IC_{50} of 391±74nM at a holding potential of -100mV, and 121±36nM at -60mV (Figure 10D).

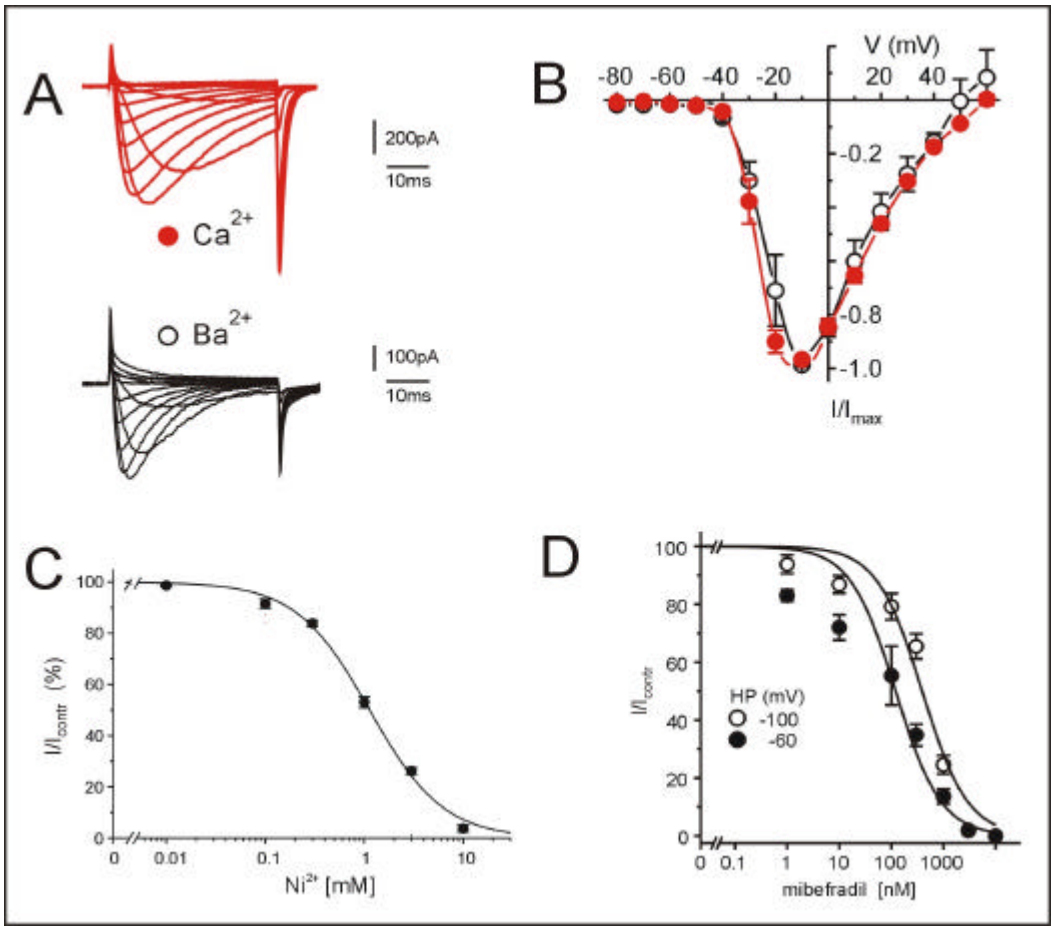

Figure 10: Characterisation of the $Ca_v3.1$ (α_{1G}) subunit by whole cell patch clamp in HEK293 cells. The typical T-type cross-over of currents is seen in representative traces of I_{Ca} and I_{Ba} (A). The current-voltage (I-V) relationship for the charge carriers, Ba^{2+}, and Ca^{2+}, is shown in (B). A 40ms long depolarising pulse was applied to the marked potentials, and the current amplitude measured. The data were normalized to the maximum current amplitude before being averaged. In (C) the inhibition of Ca^{2+} current by Ni^{2+} is plotted. The percentage of non-inhibited current amplitude versus mibefradil concentration is shown in (D), with normalized current at holding potentials of -100mVand -60mV. At least 5 cells were measured for each data point. All data are shown as mean ±SEM.

4.4.2 Electrophysiology of the γ subunits

Possible functional associations of the γ subunits with α_1 pore proteins were investigated in the HEK293 expression system, using Ba^{2+} and Ca^{2+} as charge carriers. The γ2, γ4 and γ5 subunits were co-expressed with HVA channels $Ca_v1.2$ + β2a (cardiac β), $Ca_v2.1$ + β1a (skeletal muscle variant). The β and $\alpha_2\delta$-1 subunits were co-expressed to simulate the most likely physiological complexes. γ3 was not tested, as it is 75% identical to γ2, and it is likely that they have similar biophysical properties. γ2 induced a small but significant shift in the voltage dependent activation and inactivation of the $Ca_v1.2$/β2a channel. Both γ2 and γ4 shifted the steady state inactivation curve of the $Ca_v2.1$/β1a channel to more hyperpolarizing

potentials. The $Ca_v2.1$ channel was also co-expressed with neuronal β2a, and the results were similar, except that the negative shift in the voltage dependence of inactivation was only observed when Ca^{2+} was used as a charge carrier. γ5 did not modulate the $Ca_v1.2/\beta2a$ nor the $Ca_v2.1/\beta1a$ channels. More detailed data are found in the appendix section 7.4.

The T-type $Ca_v3.1$ was also investigated for functional interactions with the γ subunits. γ4 produced a slight positive shift in the steady state inactivation curve when expressed with the T-type channel. γ5 accelerated the time course of current activation (τ_{act}) and inactivation (τ_{inact}) during a depolarizing pulse over a range of voltages, whereas γ4 only had a significant effect at certain voltages. The $\alpha_2\delta-2$ subunit was also co-expressed with the γ5 subunits, as results from the $\alpha_2\delta$ experiments indicated that it could be an interaction candidate (4.4.3.1). No additional effect of co-expression of the $\alpha_2\delta-2$ subunit was noted however.

4.4.3 Functional characterisation of the a 2d subunits

While the structure and sequence of the novel $\alpha_2\delta$ subunits suggest that they are modulatory proteins, it was necessary to test whether they have any effect on calcium current. All three subunits were expressed with several α_1 subunits and β subunits that are considered to be potential interaction partners of the pore proteins. In all cases, the co-expression of a β subunit was required for the $\alpha_2\delta$'s to have a prominent effect on the current. More detailed data are presented in the appendix (7.4).

4.4.3.1 a 2d-2a and a 2d-2b

The two splice variants of $\alpha_2\delta-2$ were co-expressed with the L-type channel $Ca_v1.2$ + cardiac β2a, as well as the non-L type channels $Ca_v2.3$ + β3 and $Ca_v2.1$ + neuronal β2a. The experiments were repeated with $\alpha_2\delta$-1 to allow for a comparison of $\alpha_2\delta$ subunits. The current density of all the HVA α_1 subunits was enhanced by expression of $\alpha_2\delta$-1, -2a and -2b. The current-voltage relationship and the steady state inactivation curves were also shifted to more negative potentials. There was no significant difference between the effects of $\alpha_2\delta$-1 and the $\alpha_2\delta$-2 subunits on $Ca_v1.2/\beta2a$. The voltage dependent activation of $Ca_v2.3/\beta3$ channel was significantly shifted in a hyperpolarizing direction by $\alpha_2\delta$-2a and -2b, but not by $\alpha_2\delta$-1. There was no difference in modulation between the two splice variants of $\alpha_2\delta$-2. However, $\alpha_2\delta$-2b, but not $\alpha_2\delta$-2a or $\alpha_2\delta$-1

shifted the voltage dependence of activation of the $Ca_v2.1/\beta2a$ channel to more negative potentials (7.4).

4.4.3.2 a$_2$d-3

The brain specific subunit, $\alpha_2\delta$-3 was co-expressed with $Ca_v1.2$ + cardiac β2a, as well as $Ca_v2.3$ + β3 in HEK293 cells, and the Ba^{2+} current measured. The $\alpha_2\delta$-3 subunit increased the current density, shifted the voltage dependence of channel activation and inactivation in a hyperpolarizing direction, and accelerated the kinetics of current inactivation of $Ca_v1.2/\beta2a$. The effects of $\alpha_2\delta$-1 and -3 on the $Ca_v1.2/\beta2a$ channel were very similar. $\alpha_2\delta$-3 had a more pronounced effect than $\alpha_2\delta$-1 when expressed with $Ca_v2.3/\beta3$. The voltage dependence of activation was shifted by $\alpha_2\delta$-3 but not by $\alpha_2\delta$-1, while $\alpha_2\delta$-3 shifted the voltage dependence of inactivation to a larger degree than $\alpha_2\delta$-1. The numerical data are shown in the appendix (7.4).

4.5 Analysis of the a$_2$d proteins

Although the $\alpha_2\delta$-1 subunit has been extensively investigated, the structure, distribution and drug-binding properties of the novel $\alpha_2\delta$ subunits have not, until now, been characterised. Using isoform specific antibodies, Western blot analyses could be performed, and information on the protein composition and tissue expression obtained. Potential binding of gabapentin to the novel subunits was also investigated, as this drug is known to bind $\alpha_2\delta$-1.

4.5.1 Specificity of the anti-a$_2$d polyclonal antibodies

In order to establish whether the $\alpha_2\delta$ protein expression correlates with that of the mRNA, as well as to study the gross structure of the proteins, antibodies against peptides of the novel subunits were produced. The specificity of the peptide antibodies was tested using membrane preparations of COS-7 cells transfected with the various $\alpha_2\delta$'s. The commercial $\alpha_2\delta$-1 antibody did not recognise $\alpha_2\delta$-2 and -3 preparations. Similarly, the peptide antibodies only recognised the $\alpha_2\delta$ against which they were raised (Figure 11A). As a further test of the antigen specificities of the antibodies, a Western blot was performed in which the antibodies were pre-incubated with an excess of the respective peptide antigen. Bands corresponding to the expected sizes for $\alpha_2\delta$-2 and –3 were detected when the antibodies were normally applied, but these bands disappeared when the

antibodies were pre-incubated with the antigen (Figure 11B). These results indicate that the antibodies are specific.

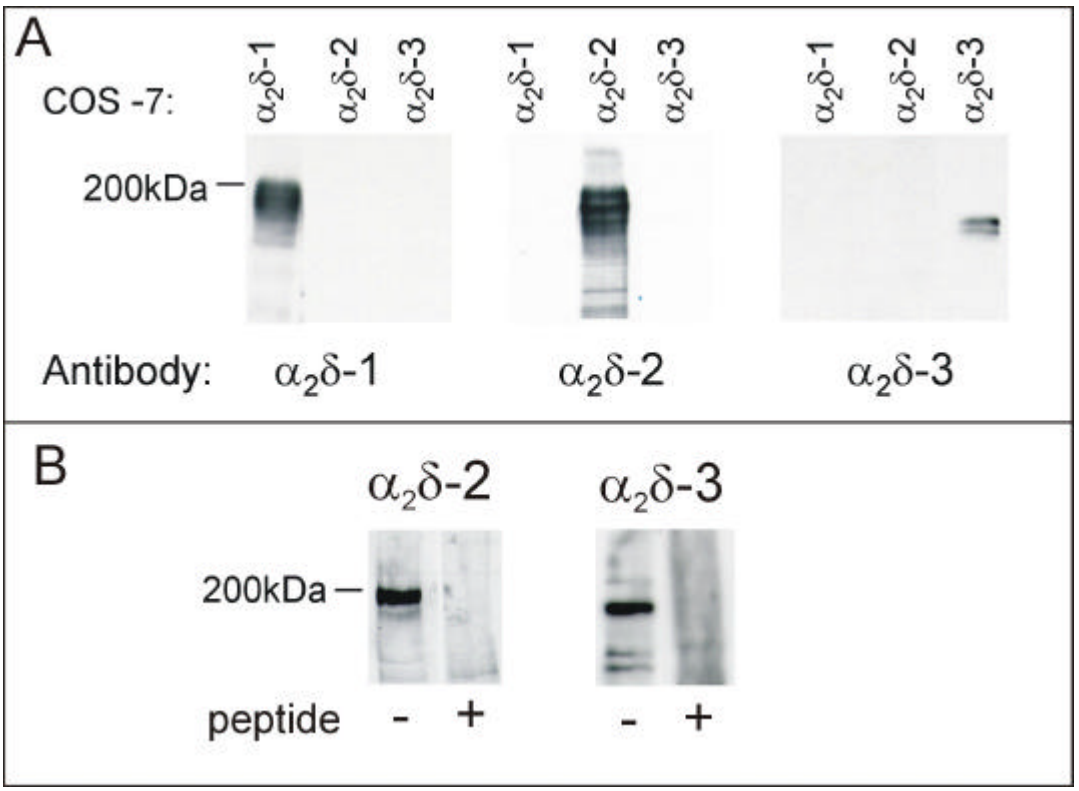

Figure 11: The anti-$\alpha_2\delta$-2 and -3 antibodies were judged to be isoform specific. Membranes from COS-7 cells transfected with the subunits were tested for reactivity in immunoblots (A). The antibodies were incubated with (+) and without (-) the antigen peptide prior to incubation with immunoblots of mouse brain membranes in order to establish whether the reactions were antigen-specific (B).

4.5.2 Immunocytochemistry

To confirm expression of the proteins in cell culture, as well as to investigate the potential use of the antibodies for immunohistochemistry, HEK293 cells were transfected with $\alpha_2\delta$-2 and -3 subunits and incubated *in situ* with the polyclonal antibodies. Both $\alpha_2\delta$-2 and -3 were expressed above backgound levels (Figure 12). Although the subunits are membrane proteins, considerable staining was also seen in the cytoplasm, with no staining in the nucleus. This is believed to be due to the high level of expression that could result in excess protein remaining in the cytoplasm, as well as the anticipated post-translational processing of the proteins in cytoplasmic structures.

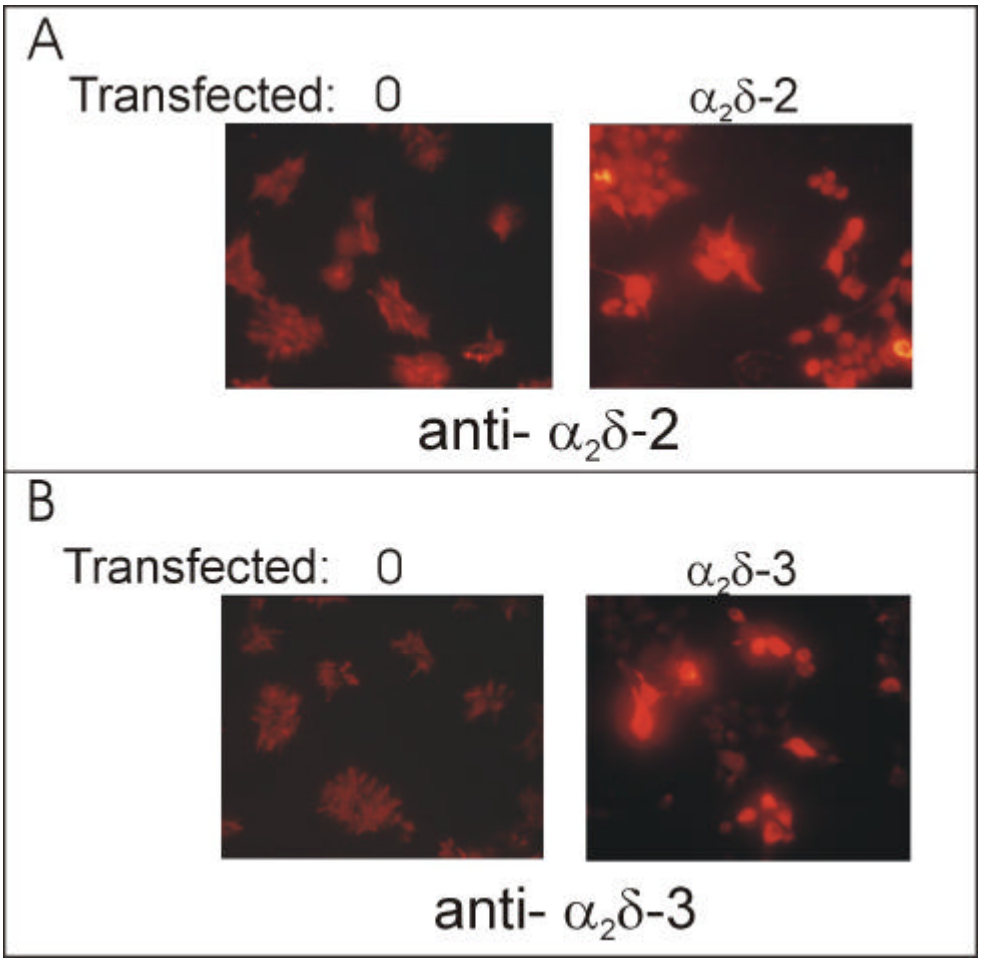

Figure 12: Immunocytochemistry of HEK293 cells transfected with the $\alpha_2\delta$-2 and -3 subunits. The primary antibodies applied were the $\alpha_2\delta$-2 and -3 antibodies, and the secondary antibody was conjugated to the fluorescent CY-3 marker. Background staining is shown in the left of the panels, and that resulting from the expression of $\alpha_2\delta$-2 (A) and $\alpha_2\delta$-3 (B) in the right side. The original magnification was 200x.

4.5.3 Post-translational modification of a $_2$d subunits

To establish whether the $\alpha_2\delta$-2 and –3 proteins are similar in structure to $\alpha_2\delta$-1, immunoblotting analyses were performed. In the first analysis the protein was reduced to establish whether the subunit consists of two separable proteins bound by disulfide bonds between the cysteine residues. The presence of oligosaccharide groups could be determined by incubating the protein with an enzyme that specifically removes N-linked sugars.

4.5.3.1 Reduction of the a $_2$d proteins

Using antibodies against all three $\alpha_2\delta$'s, various murine tissues were analysed by Western blotting. It was found that $\alpha_2\delta$-1 in brain had a mass of 200kDa under non-reducing conditions and 140kDa in a reducing environment (Figure 13A). $\alpha_2\delta$-2 in mouse brain had an apparent

molecular mass of 190kDa under non-reducing conditions, which shifted to 138kDa when DTT was added. $\alpha_2\delta$-3 in brain had the lowest mobility of the $\alpha_2\delta$ proteins, with a mass of 166kDa under non-reducing and 131kDa under reducing conditions (Figure 13A). These results indicate that, similar to $\alpha_2\delta$-1, $\alpha_2\delta$-2 and $\alpha_2\delta$-3 consist of separate, disulfide linked α_2 and δ proteins. Since the antibodies recognise the amino-terminal domains of the $\alpha_2\delta$-2 and -3 subunits, which correspond to the putative α_2, the shift in migration is due to the loss of the δ protein caused by reduction of the disulfide bonds. The mass estimated by subtraction for δ of $\alpha_2\delta$-1 is 53kDa, 57kDa for $\alpha_2\delta$-2, and 35kDa for $\alpha_2\delta$-3. A shift in electrophoretic mobility of both $\alpha_2\delta$-2 and -3 upon reduction was also observed in COS-7 membranes expressing the proteins (inset of Figure 16). The multiple bands detected are most likely due to glycosylation and processing of the overexpressed proteins by the COS-7 cells.

4.5.3.2 Deglycosylation of the a 2d proteins

To test whether the novel subunits are N-glycosylated, mouse brain membrane preparations were incubated with N-glycosidase F and analysed by Western blotting. As can be seen in Figure 13, deglycosylation resulted in the loss of approximately 30kDa for all 3 $\alpha_2\delta$'s.

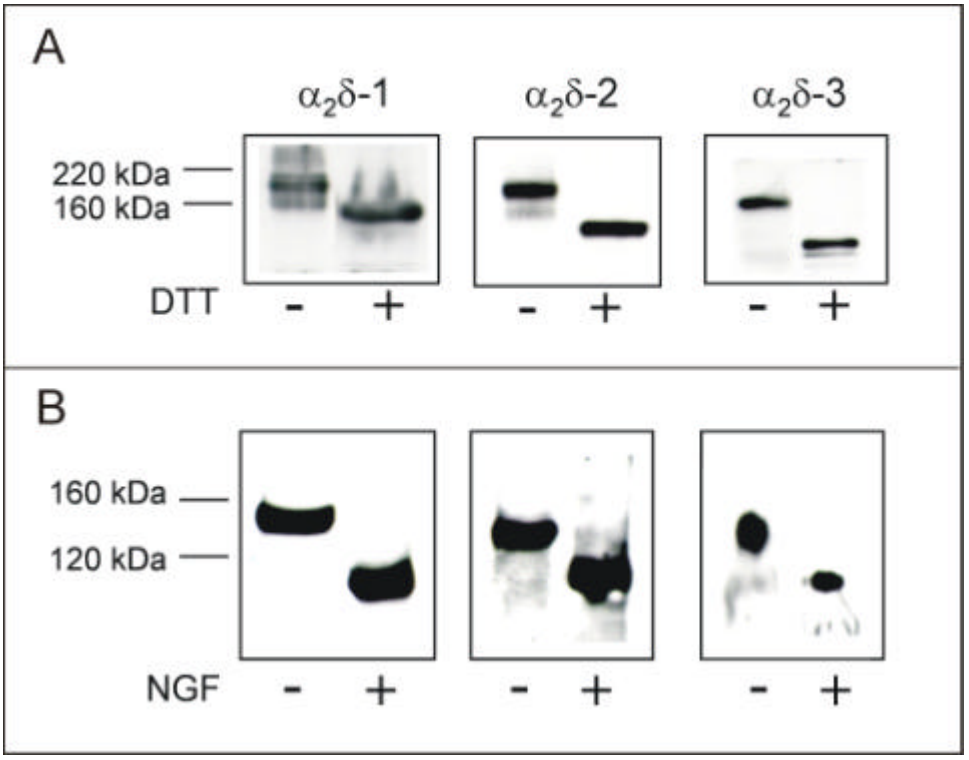

Figure 13: The $\alpha_2\delta$-2 and $\alpha_2\delta$-3 subunits are post-translationally modified. Reduction of brain membrane protein (+ **DTT**) prior to SDS-PAGE and immunoblotting results in a change in the apparent mass of all three $\alpha_2\delta$ subunits (A). Deglycosylation using **NGF** (N-glycosidase F) resulted in a loss of mass of approximately 30kDa (B).

4.5.4 Tissue distribution of $\alpha_2\delta$ subunit proteins

The tissue distribution of the three $\alpha_2\delta$ subunits in mouse was analysed by immunoblotting. As is shown in Figure 14A, $\alpha_2\delta$-1 is expressed in all tissues studied, namely brain, heart, skeletal muscle, liver and lung. The highest expression was seen in skeletal muscle and brain. It should be noted that in the latter case only 40µg of protein was used while 100µg of the other preparations were loaded. The heart subunit had a larger apparent mass than that of the brain subunit – 150 kDa as compared to 140kDa (reducing conditions).

$\alpha_2\delta$-2 was found to be expressed at high levels in brain, and to a lesser extent in heart (Figure 14B). Weaker reactive bands of a similar size were seen in lung, liver and skeletal muscle, in addition to bands at approximately 120kDa in brain, heart and lung. The apparent mass of the primary reactive band in heart was 153kDa under reducing conditions, which is larger than that seen for $\alpha_2\delta$-2 in brain (138kDa). $\alpha_2\delta$-3 was only found to be expressed in brain, and the smears below and above the size expected for $\alpha_2\delta$-3 in skeletal muscle are believed to be due to spurious reactions with contractile elements (Figure 14C).

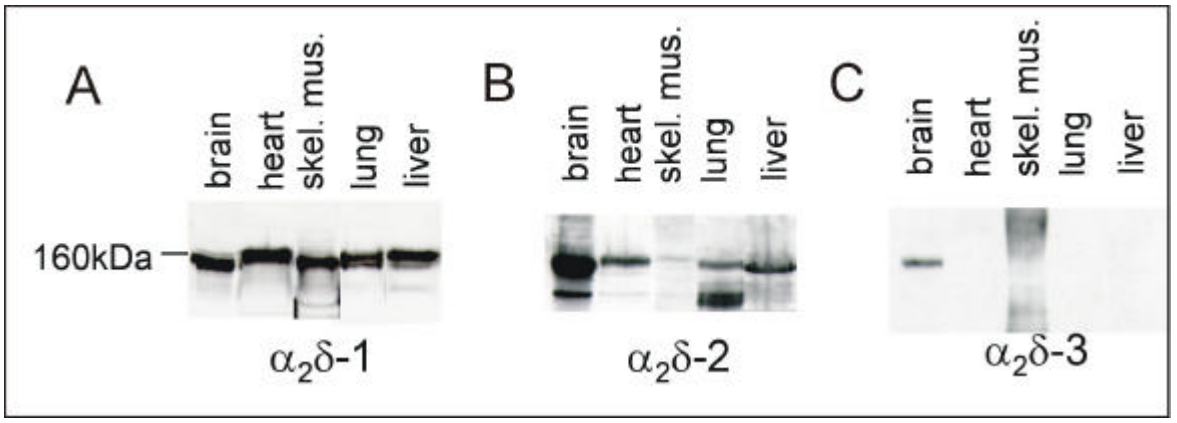

Figure 14: The tissue distribution of $\alpha_2\delta$-1 (A), $\alpha_2\delta$-2 (B) and $\alpha_2\delta$-3 (C) was established by immunoblotting. Membrane protein from the indicated murine tissues were separated by SDS-PAGE, transferred to membranes and immunoblotted. One hundred µg of protein was loaded per lane, except for skeletal muscle for the $\alpha_2\delta$-1 blot and brain for both $\alpha_2\delta$-1 and $\alpha_2\delta$-2 blots. While $\alpha_2\delta$-1 and -2 could be detected at varying levels in all the tissues tested, $\alpha_2\delta$-3 was only found in brain.

4.5.5 $\alpha_2\delta$-Myc His constructs

With a view to identifying the site of post-translational cleavage of the $\alpha_2\delta$-2 and -3 subunits, DNA constructs with a Myc-His tag were generated and expressed in COS-7 cells. The purpose of this

strategy was to purify the protein using the Myc-His tag, reduce the complex into α_2 and δ proteins, isolate δ by SDS-PAGE and sequence the amino-terminal. The amino-terminal sequence of δ could then yield information on the position of the cleavage site. Membranes of COS-7 cells transfected with the constructs were prepared, and analysed by immunoblotting. No shift in the molecular mass of $\alpha_2\delta$-2 or -3 upon reduction was observed using either the $\alpha_2\delta$ antibodies or the anti-myc antibody (Figure 15). The constructs were also expressed in HEK293 cells, with similar results. This indicates that the addition of the tag interferes with the normal processing of the proteins, and that the $\alpha_2\delta$ pre-protein is not cleaved into two separable moieties.

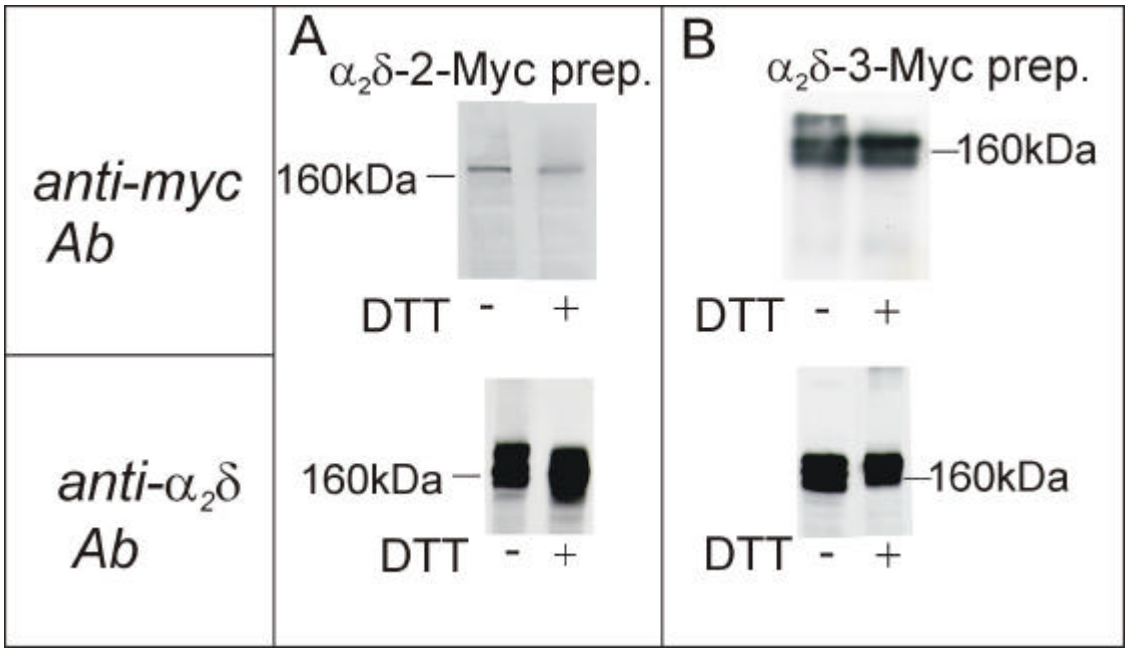

Figure 15: Addition of a Myc-His tag to $\alpha_2\delta$-2 and $\alpha_2\delta$-3 results in a failure of the protein to be cleaved into separable α_2 and δ proteins. In (A) a membrane preparation of COS-7 cells transfected with the $\alpha_2\delta$-2-Myc construct was analysed by immunoblotting with anti-$\alpha_2\delta$-2 and anti-myc antibodies. This was also done for the $\alpha_2\delta$-3-Myc preparation (B).

4.5.6 Gabapentin Binding Assays

Binding of GBP to the $\alpha_2\delta$ subunits was assessed using COS-7 cells that overexpressed the proteins. Membrane preparations were incubated with [^{3}H]-gabapentin for 30min. The protein was subsequently precipitated, captured on filters and measured by scintillation counting. $\alpha_2\delta$-1 and $\alpha_2\delta$-2 were found to specifically bind GBP while $\alpha_2\delta$-3 did not show any binding (Figure 16). Cells transfected with pcDNA3 alone did not interact with GBP.

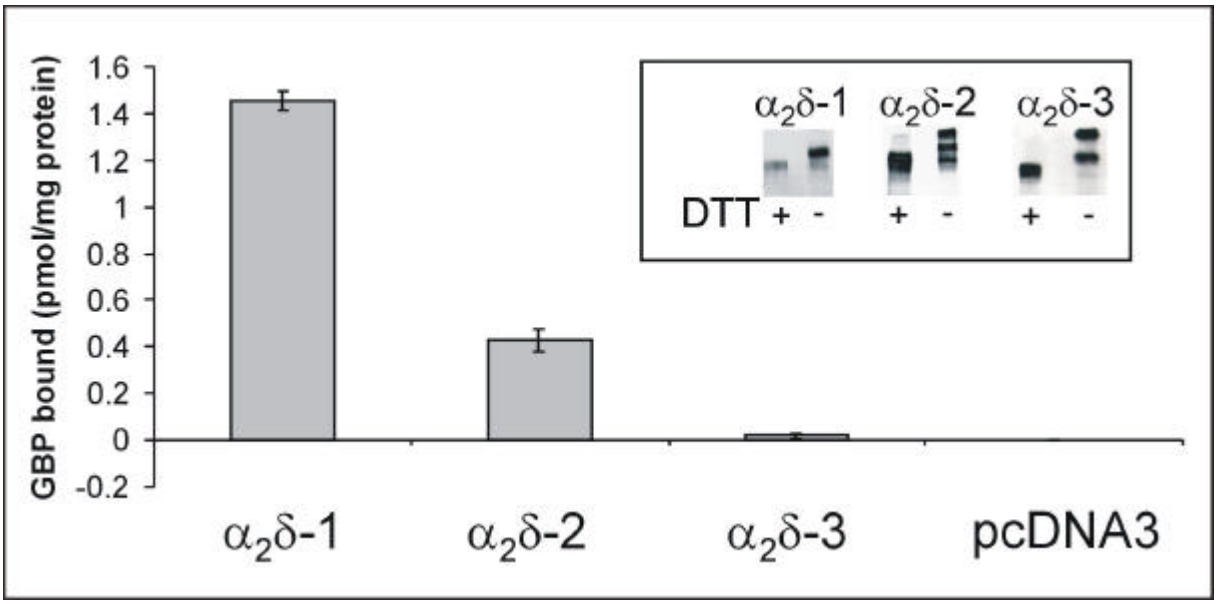

Figure 16: $\alpha_2\delta$-1 and $\alpha_2\delta$-2, but not $\alpha_2\delta$-3 bind the anti-epileptic drug gabapentin. COS-7 cells were transfected with the $\alpha_2\delta$ subunits or pcDNA3 alone. The membrane protein was prepared, incubated with 20nM [^{3}H]-gabapentin and the amount of ligand bound determined. The $\alpha_2\delta$-1 and -2 preparations bound gabapentin while the $\alpha_2\delta$-3 and empty-vector preparations did not (A). The inset shows an immunoblot of the membrane preparations used in the assays.

The $\alpha_2\delta$-1 and $\alpha_2\delta$-2 membrane preparations were further analysed by incubating the protein with varying concentrations of GBP and measuring the ligand bound. $\alpha_2\delta$-1 was found to bind to GBP with a relatively high affinity, and a dissociation constant (K_d) of 59±6nM (SEM) was calculated by Scatchard analysis of data from three experiments (Figure 17). $\alpha_2\delta$-2 was found to bind GBP with a K_d of 153±14nM (SEM) in six independent experiments. In both cases, GBP appeared to bind to a single binding site, as judged by the Scatchard plots.

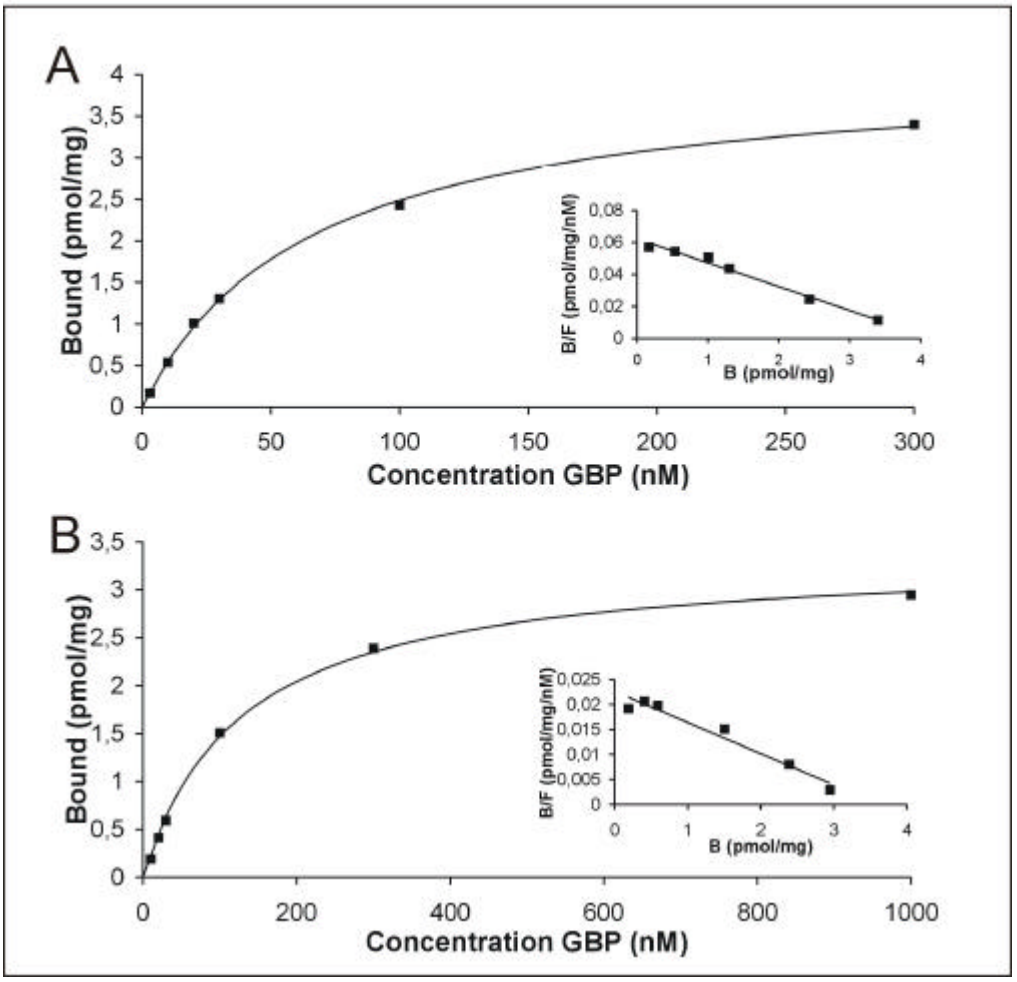

Figure 17: Gabapentin binds to $\alpha_2\delta$-1 and -2 with different affinities. Ten µg of protein was incubated with the indicated concentrations of gabapentin. A representative saturation curve for each subunit is shown, with the corresponding Scatchard plot. A K_d of 59±6nM (SEM) was calculated for $\alpha_2\delta$-1 (A) and 153±14nM (SEM) for $\alpha_2\delta$-2 (B). Three independent experiments for $\alpha_2\delta$-1 and six for $\alpha_2\delta$-2 were performed, with each assay done in duplicate. Specific binding was determined in the presence of 10µM unlabelled gabapentin

5 Discussion

The distribution of calcium channel subunits and their electrophysiological properties provide insight into the composition of calcium channels *in vivo*. The results of mRNA mapping of novel α_1 and auxiliary subunits as well as a functional analysis of these entities are discussed below. Conclusions drawn from structural and drug-binding studies of the novel $\alpha_2\delta$ proteins are subsequently presented.

5.1 Distribution and potential association of calcium channels subunits

In order to establish which voltage activated calcium channel subunits associate *in vivo*, the mRNA expression patterns were studied in various tissues. The subunit distribution in mouse brain was further investigated by *in situ* hybridisation, since calcium channels play an important role in neural excitabilty and function. An identification of potential interaction partners was possible by a comparison of subunit distribution as well as by functional characterisation of co-expressed subunits.

Northern analysis of the subunits under investigation indicated that $Ca_v3.1$ is found in several tissues, including brain (Klugbauer et al. 1999a), $\alpha_2\delta$-1 and -2 are ubiquitously expressed, while $\alpha_2\delta$-3, γ2, γ3 and γ4 are brain specific (this study, Klugbauer et al. 2000). The distribution of the neuronally expressed subunits were further analysed by *in situ* hybridisation of mouse brain slices.

Expression of $Ca_v3.1$ was found to be at its highest in cerebellar Purkinje cells, thalamus, olfactory bulb and hippocampus. These results are in agreement with those of other groups, who also showed that the protein distribution correlates closely with the mRNA expression pattern (Craig et al. 1999; Talley et al. 1999).

ISH analyses showed that the mRNA of the modulatory subunits, $\alpha_2\delta$ and γ, are expressed in several regions of the brain, with each subunit having a unique expression pattern. While γ4 and $\alpha_2\delta$-3 have high levels of expression in structures such as the caudate putamen and olfactory bulb, $\alpha_2\delta$-1 and γ2 were highly expressed in the hippocampus.

The α_1 protein forms the functional pore of the channel, and HVA α_1 subunits are known to associate with the auxiliary β, $\alpha_2\delta$ and γ subunits. It has not yet been established however, whether

preferential combinations between α_1 and these modulatory subunits occur. The distribution of the various subunits in brain were therefore compared, since an overlap of expression could suggest physiological interactions. Hypotheses regarding these proposed interactions were tested by co-expressing the proteins and analysing the channels electrophysiologically. When the ISH results of this study were compared with those of other α_1 and auxiliary subunits (Table 2) it became apparent that, while many of the subunits were complementarily expressed, an absolute overlap of expression did not occur. A number of brain regions (eg. the hippocampus and olfactory bulb) expressed several of the subunits in the same cell layers, suggesting that interactions occur in these regions. To obtain support for these proposed interactions, the subunits were co-expressed in a human cell line and studied by electrophysiological methods (5.2).

Table 2. Summary of the distribution of α_1, γ and $\alpha_2\delta$ subunits in mouse and rat brain. The relative levels of expression are indicated as (-) not detected, (+) a low level, (++) moderate expression and (+++) high levels.

	$Ca_v1.2$[1]	$Ca_v1.3$[1]	$Ca_v2.1$[1]	$Ca_v2.2$[1]	$Ca_v2.3$[2]	$Ca_v3.1$	$Ca_v3.2$[3]	$Ca_v3.3$[3]	$\alpha_2\delta$-1	$\alpha_2\delta$-2	$\alpha_2\delta$-3	γ2	γ3	γ4
Olfactory bulb	++	++	++	+	+++	++	+++	++	++	++	-	++	++	+++
Cortex	-	+	++	++	++	++	++	++	+++	+	++	++	++	-
Hippocampus														
Ammon's horn	++	+	+++	++	+++	++	+++	++	+++	-	+++	++	++	-
Dentate gyrus	++	++	+++	++	+++	+	++	+	+++	-	+++	-	-	-
Caudate putamen	-	-	+++	+	+++	-	++	+	+	-	+++	+	-	+++
Cerebellum														
Molecular layer	-	-	++	-	-	+	-	-	-	+	++	-	-	-
Purkinje layer	-	++	+++	-	+++	+++	-	-	-	+++	-	+++	-	++
Granular layer	++	++	+++	++	+++	+	-	+	++	+	+	-	-	-
Thalamus	+	-	++	++	+	++	+	+	+	++	+	++	-	++

Sources of mRNA localisation data not presented in this thesis :
1 – Ludwig et al. (1997), 2 - Soong et al. (1993), 3 – Talley et al. (1999)

5.2 Functional characterisation

In order to confirm that the novel α_1 subunit cloned was in fact a LVA channel, the electrophysiological characteristics of mouse $Ca_v3.1$ were investigated by whole cell patch clamp experiments in HEK293 cells. The voltage dependence and kinetics of activation and inactivation, as well as the mibefradil sensitivity of the expressed pore subunit were similar to that described for rat $Ca_v3.1$ and (Perez-Reyes et al. 1998) and native T-type current (for review see Huguenard, 1996)

The γ subunits were expressed with several α_1 and β subunits and the current and conductance analysed. The modulatory effects of the γ subunits on the channels expressed were modest, with only slight changes in the electrophysiology of the α_1-β combinations noted. The $\gamma 2$ results are in agreement of those of Letts (1998), and it was found that $\gamma 4$ behaves similarly. $\gamma 5$ is a possible candidate for interaction with $Ca_v3.1$, as it induced small, but significant changes in a number of current properties. It is likely that $\gamma 2$ has other functions in brain, since a recent report (Chen et al., 2001) shows this protein to be essential for the synaptic targeting of AMPA (α-amino-3-hydroxyl-5-methyl-4-isoxazoleproprionate) receptors to postsynaptic membranes of cerebellar granule cells. AMPA receptors bind the neurotransmitter glutamate and are important for transduction of excitatory signals in neurons. Since $\gamma 3$ and $\gamma 4$ are 76% and 60% homologous to $\gamma 2$, respectively, these proteins could also have additional roles in neuronal function. The functions of the neuronal γ subunits remain to be clarified, and the links between voltage gated calcium channels and neurotransmitter receptors established.

To infer which subunits form the most likely physiological partners for the novel $\alpha_2\delta$ subunits, they were co-expressed with various α_1 subunits and studied electrophysiologically. $\alpha_2\delta$-2 and -3 were both found to significantly enhance and modulate the current through the HVA channels $Ca_v1.2$ and $Ca_v2.3$. These effects were only distinguishable from those of $\alpha_2\delta-1$ in the case of $Ca_v2.3$, suggesting a preferential interaction of this α_1 protein with the novel subunits. Of the $\alpha_2\delta$ subunits, $\alpha_2\delta$-2 (both splice variants) had the most prominent functional effect on the current conducted through $Ca_v2.1$, and may preferentially associate with it. Interestingly, $\alpha_2\delta$-2 (both splice variants) may associate with $Ca_v3.1$, a LVA channel that has not yet been demonstrated to bind other proteins. Gao and co-workers (2000) reported that $\alpha_2\delta$-2 may associate with rat $Ca_v3.1$, but

whereas this group found only an increase in the current amplitude, our study indicated that other biophysical characteristics are also altered.

One of the sources of neural plasticity is the diversity of voltage gated calcium channel types. In addition to region-specific interactions between subunits, it is likely that a concentration effect could occur in cells where multiple forms of each subunit are expressed. For example the pyramidal neurons of the hippocampus express $Ca_v1.2$, $Ca_v1.3$, $Ca_v2.1$, $Ca_v2.2$, $Ca_v2.3$, $Ca_v3.1$, $Ca_v3.2$ and $Ca_v3.3$, all 4 β's, $\alpha_2\delta$-1 and -3, γ2 and γ4. An abundantly expressed subunit could dominantly form complexes with other subunits, although the interactions between these subunits may not be the strongest. The origin of calcium channel complexity are thus severalfold. Firstly, developmental or temporal fluctuations in expression levels would determine the channel composition. Secondly, a regional and cell type specific expression would restrict associations. Thirdly, differences in the distribution within a cell could dictate current properties in a microenvironment. Finally, the concentrations of the subunit may contribute to determining which channel complexes are formed *in vivo*.

5.3 a$_2$d protein and drug binding analyses

In studies designed to elucidate the structure and properties of the novel $\alpha_2\delta$-2 and -3 subunits, immunoblotting and drug binding analyses were undertaken. Peptide antibodies were raised against $\alpha_2\delta$-2 and -3 in order to yield information on the structure and distribution of the proteins. Radioligand binding assays were also peformed to establish whether these subunits bound gabapentin, a drug used for neurological disorders that is known to bind $\alpha_2\delta$-1.

5.3.1 Structure and post-translational modifications of the a$_2$d proteins

By directing the polyclonal antibodies against the putative α_2 of the $\alpha_2\delta$-2 and -3 subunits, it could be assessed by Western blotting whether the precursor proteins are cleaved into α_2 and δ and if these proteins are subsequently disulfide-linked. Both $\alpha_2\delta$-2 and -3 in native tissue were found to be composed of an α_2 and δ, which could be separated by reduction. The difference in mass of the non-reduced complex relative to the reduced protein roughly corresponds to that of δ alone and was approximately 50kDa for each of the $\alpha_2\delta$'s. The cleavage site of $\alpha_2\delta$-1 is between A^{934} and A^{935},

when the signal sequence is not taken as part of the protein (De Jongh et al., 1990, Jay et al. 1991). The alanine at position 934 in $\alpha_2\delta$-1 is conserved in $\alpha_2\delta$-2 and -3, although the rest of the sequence in the region diverges (Figure 18). While the $\alpha_2\delta$-1 cleavage site cannot be assumed to be the same as for the novel proteins, the approximate sizes of the δ's and the conservation of the alanine suggest that this could be the case. If the alanine is assumed to be the first residue of δ for both $\alpha_2\delta$-2 and -3, then the mass calculated for δ of $\alpha_2\delta$-2 based on its amino acid content is 17.2kDa, and for $\alpha_2\delta$-3, 15.1kDa. The mass estimated indirectly is larger than that calculated using the amino acid sequence. This difference is likely to be due to the difficulty associated with inferring sizes based on shifts in SDS-PAGE migration of reduced and non-reduced proteins, as well as post-translational modifications such as N-glycosylation (both δ proteins contain potential N-glycosylation sites). A similar pattern of modification has been observed for the δ of $\alpha_2\delta$-1 which has a calculated mass of 19kDa, and a migration of 24 and 27kDa using antibodies against the δ (De Jongh et al., 1990).

The addition of a Myc-His tag to the $\alpha_2\delta$'s led to a failure in the processing of the proteins, as they were not cleaved into α_2 and δ. A similar phenomenon was noted by Wang and colleagues (1999), where the deletion of the 7 amino acids closest to the carboxy terminal of δ led to aberrant cleavage. This suggests that the carboxy terminal is essential for correct proteolysis, perhaps by forming an essential folding structure or protease recognition motif. Alternatively, $\alpha_2\delta$ could itself be a protease, with the carboxy terminal involved in the cleavage of the precursor protein. This is unlikely however, as the amino acid similarity in this region is low.

$\alpha_2\delta$-2 and -3 were shown to be similar to $\alpha_2\delta$-1 in terms of glycosylation, with 30kDa of the mass of the proteins consisting of oligosaccharides. Since glycosylation is essential for current stimulation by $\alpha_2\delta$-1 of $Ca_v2.1$ (Gurnett et al., 1996), this is likely to be the case for the novel subunits as well.

5.3.2 Distribution of the $\alpha_2\delta$'s in murine tissues

The distribution of $\alpha_2\delta$ protein in mouse tissues was compared with that of the mRNA expression pattern (Klugbauer et al., 1999a). As anticipated from the dot blot data, $\alpha_2\delta$-1 was found to be ubiquitously expressed. The highest protein levels were observed in skeletal muscle and brain, which is in line with the mRNA expression. $\alpha_2\delta$-3 was only detected in brain, which corresponds to the results of the Northern analysis. $\alpha_2\delta$-2 mRNA was originally described as being ubiquitously

expressed, with the highest levels in brain, heart, pancreas and skeletal muscle (Klugbauer et al., 1999a). Lower levels of the mRNA were seen in other tissues after longer exposures. In this study $\alpha_2\delta$-2 protein was detected at very low levels in skeletal muscle, although the Northern analysis had produced a signal comparable to brain. Gao and co-workers (2000) reported high levels of $\alpha_2\delta$-2 mRNA in human lung, and cloned the subunit from a lung library. Although $\alpha_2\delta$-2 protein was observed at low levels in mouse lung in this study, it is possible that certain lung cell types express high levels. While the Gao group showed overexpression of $\alpha_2\delta$-2 protein in various tumour cell lines, no data was presented on the endogenous levels in healthy lung tissue.

The size of $\alpha_2\delta$-1 estimated by SDS-PAGE is in accord with that reported previously (Jay et al., 1991). However, heart $\alpha_2\delta$-1 had a larger apparent mass of 150kDa under reducing conditions, compared to that of brain (140kDa). The $\alpha_2\delta$-1b splice variant is exclusively found in brain, while the predominant forms in heart are $\alpha_2\delta$-1c and -d (Angelotti and Hofmann, 1996). Since the $\alpha_2\delta$-1c and -d heart splice variants have 5 and 12 fewer amino acids than that of the brain isoform, respecively, the difference in mass is believed to be due to glycosylation.

Two reactive bands were observed for $\alpha_2\delta$-2. This may also be due to differential glycosylation and/or splice variation, since four splice variants have been described so far for $\alpha_2\delta$-2 (Hobom et al., 2000; Gao et al., 2000). Since the antibody recognised both bands, the protein detected at lower masses probably results from the presence of more than one splice form in a tissue, partial degradation or incompletely processed forms of the highly glycosylated protein. The latter option is probable as the membrane preparations also contain endoplasmic reticulum with associated protein.

5.3.3 Gabapentin binding

Since GBP, a drug increasingly used for neurological disorders, binds to $\alpha_2\delta$-1, the novel subunits were also tested for drug binding. The K_d of purified porcine brain $\alpha_2\delta$-1 was reported as 9.4nM (Brown et al., 1998) but as 37.5nM for porcine $\alpha_2\delta$-1 expressed in COS-7 cells (Brown and Gee, 1998) and 16nM for rabbit $\alpha_2\delta$-1 also in COS-7 cells (Gee et al., 1996). In this study a K_d of 59nM for $\alpha_2\delta$-1 was determined. The reason for the variation in K_d values is not clear, but may be due to differences in the membrane preparation and binding assays. GBP was found to bind to a single set of sites in $\alpha_2\delta$-2 with a K_d of 153nM. Since GBP is used for a variety of disorders, it is

interesting to note that it binds to two auxiliary calcium channel subunits which have been found to exert differing modulatory effects on α_1 pore subunits in expression systems.

The effect of GBP on the physiological activity of calcium channels is not clearly understood. In patch-clamp studies with hippocampal granule cells, no effect of GBP was reported (Schumacher et al., 1998). However, in other studies modest to dramatic changes in calcium current were noted. A reduction in the calcium current in isolated neurons (Stefani et al., 1998) and in rat neocortical slices (Fink et al., 2000) upon application of GBP has been described. Calabresi and colleagues (2000) found that GBP reduces most excitatory properties of striatal spiny neurons, which could account for the anticonvulsant effect of the drug. Dooley and co-workers (2000) have also shown that GBP and a related compound, pregabalin, reduce the release of norepinephrine when stimulated by potassium and electrical pulses (Dooley et al, 2000). The calcium channels affected are not known, with candidates being L-type (Stefani et al., 1998) and P/Q (Fink et al., 2000, Meder and Dooley, 2000). No consistent effects of GBP on $Ca_v1.2$, $Ca_v2.1$ and $Ca_v3.2$ currents in HEK293 cells were observed in this study. The complexity of the interaction between GBP and $\alpha_2\delta$ is further illustrated by a temperature dependent influence of ruthenium red, $MgCl_2$ and spermine on GBP binding (Taylor et al., 2000). Initial studies on GBP binding using rat tissue homogenates showed strong binding in skeletal muscle and brain, where $\alpha_2\delta$-1 is most highly expressed (Gee et al., 1996). A much lower binding of the drug was seen in liver and kidney, which express considerable levels of the protein, as judged by Western blotting.

A possible explanation for these conflicting results is that the binding of GBP to $\alpha_2\delta$ is modulated by other subunits, for example the α_1 pore protein. The lack of clinical side effects of the drug on skeletal muscle and other $\alpha_2\delta$-1 expressing tissues supports this view (Beydoun et al. 1995). The clinical effects of GBP could be due to the drug interacting with a subpopulation of calcium channels under conditions that may be difficult to measure electrophysiologically. Subtle effects, such as the long-term stability of channels in the membrane, coupling of the channels to other intracellular constituents, or interactions of the drug with $GABA_B$ receptors may be responsible for the therapeutic mechanisms of GBP.

Gabapentin binding is dependent on the presence of both α and δ subunits, which do not have to be translated as a single precursor protein (Wang et al., 1999). Their interaction is important however,

as neither α nor δ bind the drug when expressed alone (Wang et al., 1999). Cleavage of the precursor protein is also not required for binding (Brown and Gee, 1998). Mutation analysis of porcine $\alpha_2\delta$-1 by Brown and co-workers (1998) led to the identification of a region (960-994) in δ-1, containing a zinc-finger like motif, that is important for gabapentin binding. Another study identified residues 206-222, 516-537 and 383-603 as being essential for binding (Wang et al., 1999). Since $\alpha_2\delta$-2 has in this study been shown to bind gabapentin, it is instructive to compare the sequences identified as putative binding sites in previous reports (Figure 18). Mutations of charged amino acids in $\alpha_2\delta$-1 was performed by Wang and colleagues, and Arg^{217} found to be the most important. This residue is found in $\alpha_2\delta$-2, but not in $\alpha_2\delta$-3, supporting its role in the binding of GBP. It is however not clear whether these sites are essential for the association of α_2 with δ, or whether they form a gabapentin binding pocket. Gabapentin analogs have been developed that bind to $\alpha_2\delta$-1 with a higher affinity than gabapentin and are effective in an animal model of epilepsy (Bryans et al., 1998). To understand the action of these drugs on calcium channels it will be important to identify the sites of interaction and determine whether these substances also interact with $\alpha_2\delta$-2 and -3.

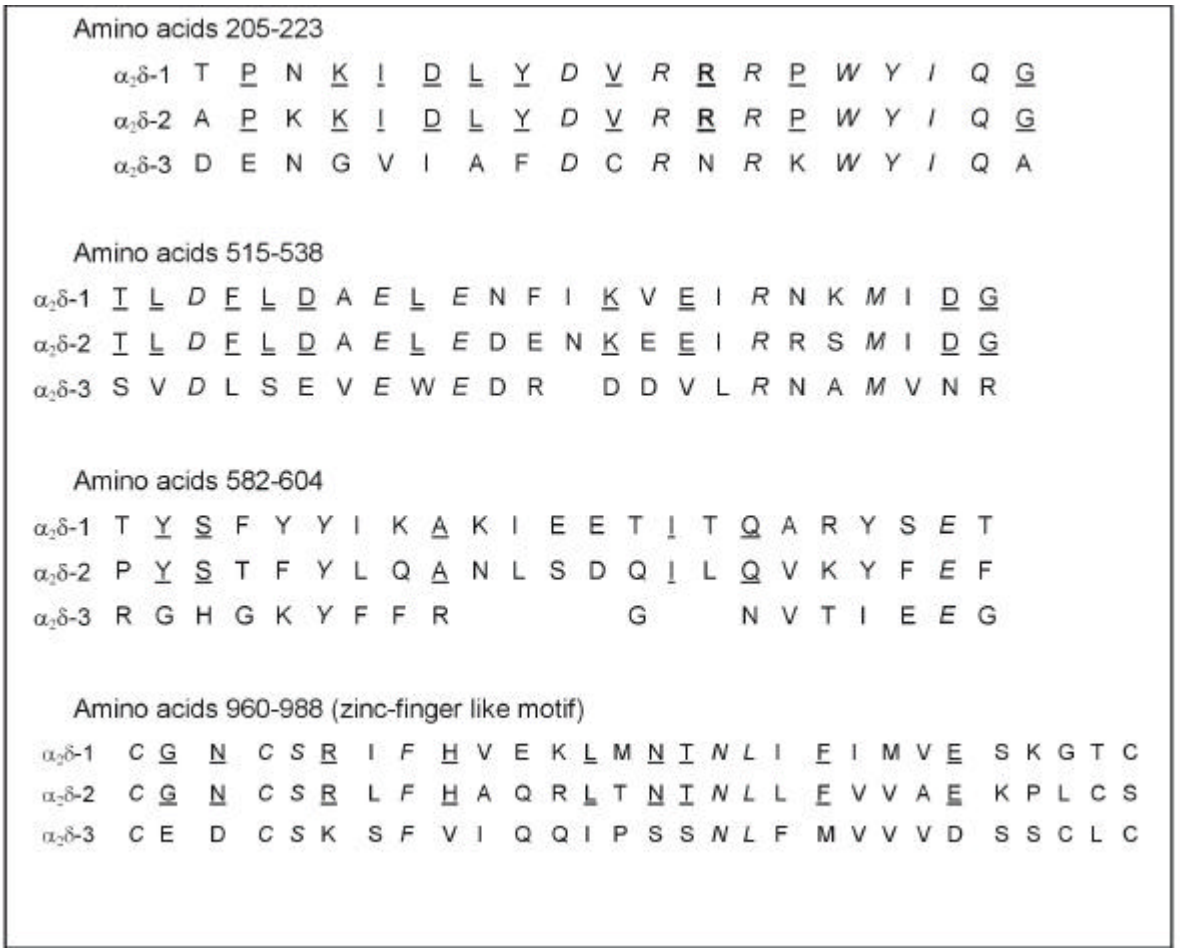

Figure 18: Alignment of $\alpha_2\delta$ sequences important for GBP binding. $\alpha_2\delta$-1 is compared with $\alpha_2\delta$-2 and $\alpha_2\delta$-3 in the regions found to be involved in GBP binding (Brown et al. 1998, Wang et al 1999). Residues conserved in $\alpha_2\delta$-1, $\alpha_2\delta$-2 and $\alpha_2\delta$-3 are in italics. Residues found only in $\alpha_2\delta$-1 and $\alpha_2\delta$-2 are underlined. Arg^{217} is shown in bold. The alignment of the sequences was done using Clustal V.

6 Summary

Voltage gated calcium channels are multimeric complexes that play an essential role in numerous physiological processes. A large family of these channels exist that differ in their voltage sensitivities and current properties. This diversity is a result of the multiplicity of subunit proteins that combine to form the calcium channel, as well as the differential protein localisation. In this thesis, the identification of subunits that interact *in vivo* was undertaken using distribution and functional analyses of the channels. The distribution of novel subunits cloned in our laboratory ($Ca_v3.1$, γ3, γ4, $\alpha_2\delta$-2 and $\alpha_2\delta$-3) in mouse brain was determined by *in situ* hybridisation and compared to that of previously characterised subunits. The novel subunits were co-expressed with potential partners in HEK293 cells and the channel properties investigated by electrophysiological techniques. The *in situ* hybridisation and electrophysiological data indicated that $\alpha_2\delta$-2 and -3 may preferentially modulate $Ca_v2.3$ and $Ca_v2.1$ in the regions of the brain where they are both expressed. The neuronal γ4 subunit could similarly regulate current through $Ca_v2.1$. $\alpha_2\delta$-2 and γ5 may be potential partners of $Ca_v3.1$, an LVA channel that has as yet not been well characterised.

In a second set of studies, the gross structures of the two novel $\alpha_2\delta$ proteins ($\alpha_2\delta$-2 and –3) were elucidated and are presented here for the first time. Western blotting analyses indicate that $\alpha_2\delta$-2 and -3 consist of two proteins that are derived from a single transcript. These proteins associate through disulfide bonding following post-translational cleavage. Similar to $\alpha_2\delta$-1, these proteins are highly N-glycosylated. The tissue distribution and relative expression levels of the proteins varies, with $\alpha_2\delta$-1 and -2 being ubiquitously expressed, and $\alpha_2\delta$-3 found only in brain.

A trait of the $\alpha_2\delta$-1 protein is its ability to bind gabapentin (GBP), a drug increasingly used for neurological disorders. Although drug binding to the α_1 subunits has been previously described, the binding of GBP to $\alpha_2\delta$-1 is the first described interaction between a regulatory subunit and a pharmaceutical agent. Binding of GBP to the $\alpha_2\delta$-2 and $\alpha_2\delta$-3 proteins was investigated in this study by radioligand assays. It was found that $\alpha_2\delta$-2 but not $\alpha_2\delta$-3 is capable of binding GBP. The affinity constant of $\alpha_2\delta$-1 for GBP was calculated to be 59nM, and that of $\alpha_2\delta$-2, 153nM. Since $\alpha_2\delta$ subunits may associate preferentially with different α_1 subunits in the brain, GBP could have varying therapeutic mechanisms if more than one of $\alpha_2\delta$ family binds the drug. The characterisation of the $\alpha_2\delta$ proteins is essential not only for understanding the clinical action of GBP, but has

implications for other pathologies. An association of $\alpha_2\delta$-2 with tumours has been suggested, and the mouse homolog is a candidate for the *ducky* epileptic phenotype (Burgess and Noebels 1999, Gao et al., 2000,).

7 Appendix

7.1 Alignment of the a_2d and g sequences

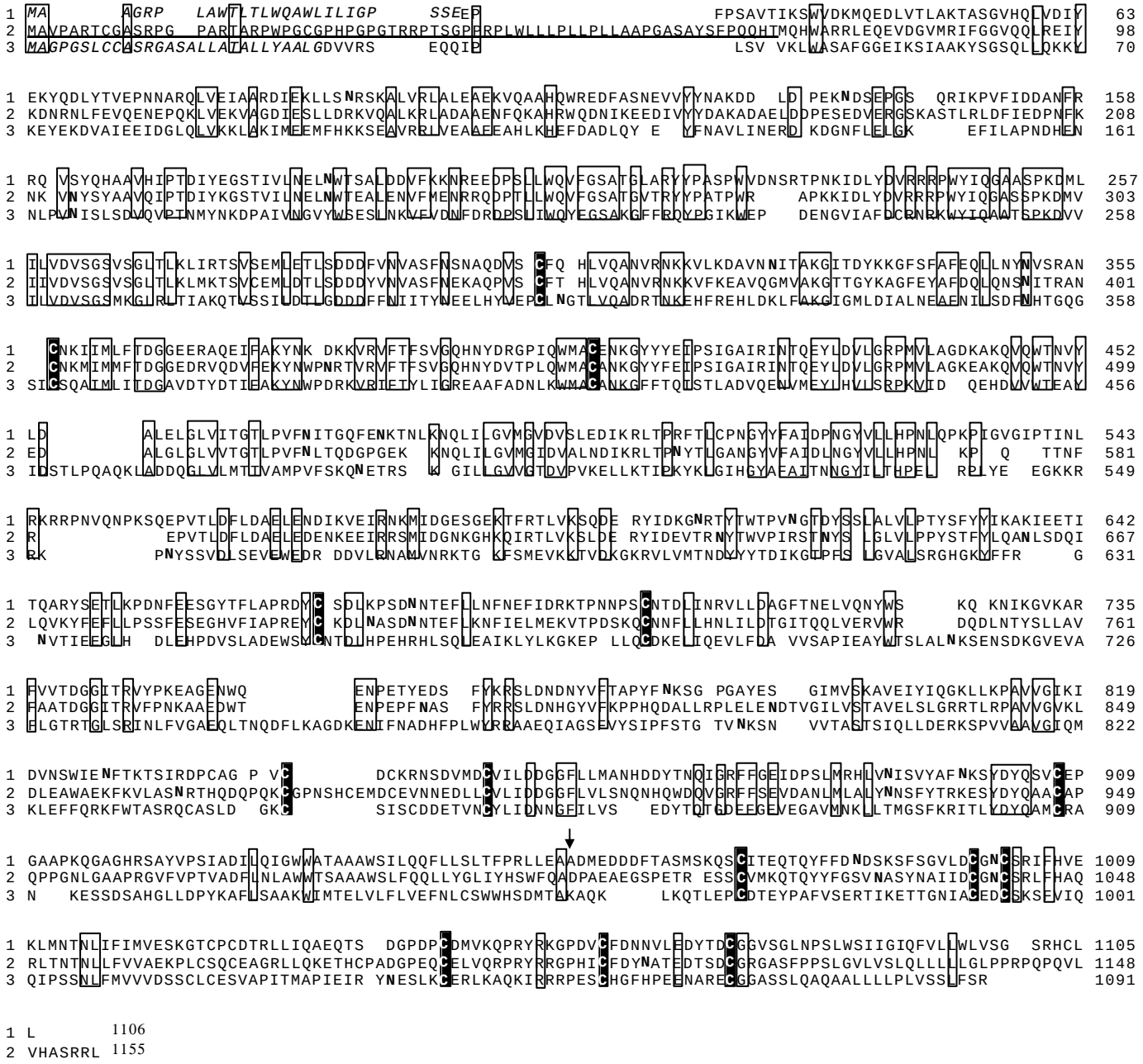

Figure 19: Alignment of the amino acid sequences of the $\alpha_2\delta$ subunits. Residues in blocks are conserved in all three sequences, and the black boxes indicate the positions of conserved cysteine residues. The arrow marks the cleavage site of $\alpha_2\delta$–1

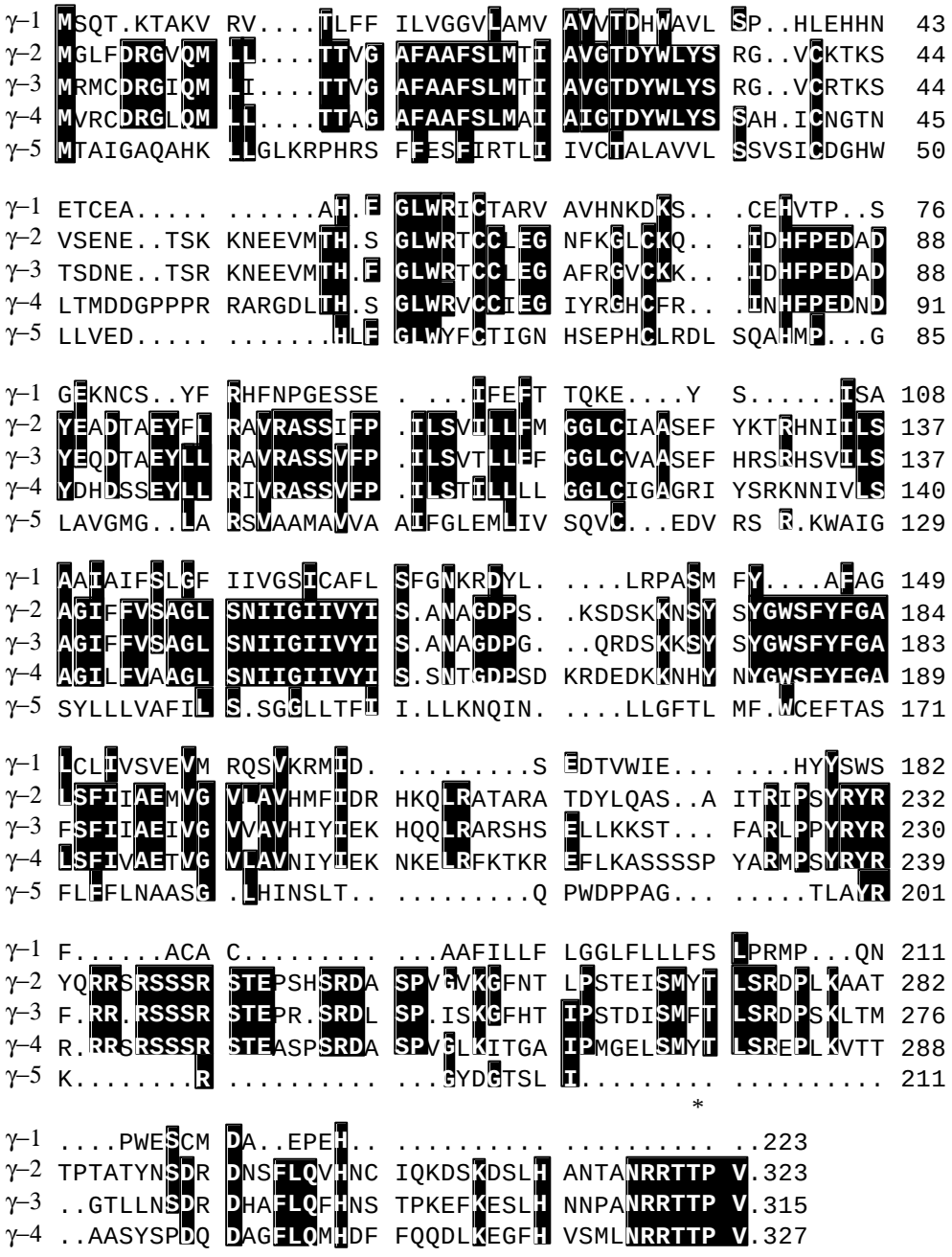

Figure 20: Alignment of the γ subunit amino acid sequences. Sequences conserved between three or more subunits are shown on a black background.

7.2 Accession numbers

Genbank accession numbers for subunits cloned and studied in our laboratory are:

$Ca_v3.1$	AJ012569
$\alpha_2\delta$-2a	AJ251367
$\alpha_2\delta$-2b	AJ251368
$\alpha_2\delta$-3	AJ010949
γ3	AJ272044
γ4	AJ272045
γ5	AJ272046

Accession numbers of subunits previously cloned, but used in this study:

$\alpha_2\delta$-1	M21948
γ1	NP062128
γ2	AF077739

7.3 PCR Primers

The primers used for amplification of *in situ* hybridisation and Northern blotting probes, as well as for the alteration of sequences are shown below. Sequences in bold indicate where restriction sites were added to allow for sticky-end cloning.

Subunit	Purpose	Primer name	Primer sequence (5' - 3')
$\alpha_2\delta$-1	ISH Dot blot	EM10	**CGC GGA TC**C TCT ATT CTC CAG CAG CTG-
		EM11	**ATT GGT ACC** CCC AGA AAC ACC ACC ACA
$\alpha_2\delta$-3	ISH	AD13	CAG TGC CCA TGG ACT TC
		AD14	CCA GGG CCT GAA GAC TCG TT
$Ca_v3.1$	ISH	EM4	CAT GCC CAG GAT GCT GAA GAT
		LVA4	CTC CCC TCT GGC TCA GA
γ2	ISH	G2F	**CGC GGA TCC** GTA GGG ACC CCC TGA AGG CTG
		G2R	**ATT GGT ACC** GGC TGT GTT GGC GTG CAG
γ4	ISH	G3F	**CGC GGA TCC** CAG AGA ACC CCT TAA GGT GAC
		G3R	**ATT GGT ACC** CAG CAT GCT GAC ATC GAA ACC
$\alpha_2\delta$-2	Myc-His constructs	a2d2His1	CAG TGG TGG GCG TCA AGC
		a2d2His2	**TAA TCT CGA G**GC GGC CAG AGG CGT CCA C
$\alpha_2\delta$-3	Myc-His constructs	a2d3His1	AGT CCG TGG CTC CTA TAA
		a2d3His2	**TAA TGG GCC CTC TAG A**CC TTG AGA AGA GAC TCG

7.4 Electrophysiological data

The electrophysiological data that were the basis for the results presented in this thesis are shown below. The subunit headings indicate which subunits were transiently transfected into HEK293 cells. The electrophysiological parameters are listed in the leftmost column. I_{Ba} and I_{Ca} are the current densities, and are shown as negative values since the current is inwards. $V_{0.5act}$ is the half-maximal activation potential, $V_{0.5inact}$ the half-maximal inactivation potential, k_{act} and k_{inact} are the kinetics of activation and inactivation, respectively. τ is the time constant of recovery from voltage dependent inactivation, with $\tau 1$ being the fast component and $\tau 2$ the slow component. Asterisks indicate values that differ significantly from the channel expressed without auxiliary subunits: * $P < 0.5$, ** $P < 0.1$ and *** $P < 0.01$. The sample size of the measurements varied between 8 and 25 cells. These data were published in Klugbauer et al. 1999a, Klugbauer et al. 1999b, Hobom et al. 1999 and Lacinová et al. 1999.

Effects of the γ2, γ4 and γ5 subunits on the activation and inactivation of $Ca_v1.2/\beta 2a$ and $Ca_v2.1/n\beta 2a$ calcium channels. 10mM Ba^{2+} was used as the charge carrier

	$Ca_v1.2$ β2a	$Ca_v1.2$ β2a $\alpha_2\delta$-1 γ2	$Ca_v1.2$ β2a $\alpha_2\delta$-1 γ5	$Ca_v2.1n\beta 2a$ $\alpha_2\delta$-1	$Ca_v2.1n\beta 2a$ $\alpha_2\delta$-1 γ2
I_{Ba} density (pA/pF)	-62.8±7.0	-45.1±8.2	-59.9±9.7	-45.9±8.8	-46.5±6.2
$V_{0.5act}$ (mV)	2.0±0.4	7.3±0.3*	1.9±0.4	6.9±0.4	7.3±0.3
k_{act}(mV)	5.9±0.2	6.1±0.2	6.2±0.3	4.4±0.2	4.5±0.2
$V_{0.5\ inact}$ (mV)	-19.8±0.6	-16.5±0.7*	-17.2±0.6	-6.5±0.5	-1.9±0.7*
k_{inact} (mV)	9.8±0.6	11.2±0.6	9.1±0.5	6.9±0.4	7.0±0.6

Effects of the γ2, γ4 and γ5 subunits on the activation and inactivation of $Ca_v2.1/\beta 1a$ and $Ca_v2.1/\beta 2a$ channels. 10mM Ca^{2+} was used as the charge carrier.

	$Ca_v2.1\beta 1a$ $\alpha_2\delta$-1	$Ca_v2.1\beta 1a$ $\alpha_2\delta$-1 γ2	$Ca_v2.1\beta 1a$ $\alpha_2\delta$-1 γ4	$Ca_v2.1\beta 1a$ $\alpha_2\delta$-1 γ5	$Ca_v2.1\beta 2a$ $\alpha_2\delta$-1	$Ca_v2.1\beta 2a$ $\alpha_2\delta$-1 γ2
I_{Ba} density (pA/pF)	-34.8±8.7	-29.9±3.4	-35.9±9.3	-36.0±8.9	-40.8±2.7	-42.9±8.4
$V_{0.5act}$ (mV)	11.9±0.1	15.0±0.1*	10.8±0.2	11.3±0.2	13.9±0.2	12.4±0.1
k_{act} (mV)	4.5±0.1	4.4±0.1	4.2±0.2	4.3±0.2	3.8±0.1	3.9±0.1
$V_{0.5inact}$ (mV)	-15.0±0.3	-18.7±0.4*	-20.0±0.3*	-14.9±0.2	4.6±0.5	1.3±.0.8*
k_{inact} (mV)	6.9±0.2	6.3±0.4	6.3±0.3	6.9±0.2	3.6±0.3	4.6±0.7

Effects of the γ2, γ4 and γ5 subunits on the activation and inactivation of $Ca_v3.1$ channel. 10mM Ca^{2+} was used as the charge carrier.

	$Ca_v3.1$	$Ca_v3.1$ γ2	$Ca_v3.1$ γ4	$Ca_v3.1$ γ5	$Ca_v3.1$ $\alpha_2\delta$-2	$Ca_v3.1$ $\alpha_2\delta$-2 γ2
I_{Ba} density (pA/pF)	-62.7±7	-87±13	-79±12	-73±9	-93±15*	-85±12
$V_{0.5act}$ (mV)	-24.9±1.2	-24.4±1.6	-23.9±1.3	-24.1±1.0	-22.3±0.8	-21.4±1.1
k_{act} (mV)	3.9±0.3	3.8±0.2	4.1±0.2	3.9±0.2	4.1±0.2	4.2±0.2
$V_{0.5inact}$ (mV)	-54.9±1.2	-51.4±1.4	-50.0±1.4*	-51.7±1.2	-50.4±0.7**	-49.3±1.1**
k_{inact} (mV)	4.3±0.2	4.2±0.2	3.9±0.2	4.5±0.2	4.0±0.2	4.1±0.3
τ (ms)	251±24	336±14**	320±17*	248±11	279±12	296±25

Effects of the $\alpha_2\delta$-1 and 3 subunit on the activation and inactivation of the HVA calcium channels, $Ca_v1.2$/β2a and $Ca_v2.3$/β3. 20mM Ba^{2+} was used as the charge carrier

	$Ca_v1.2$β2a	$Ca_v1.2$ β2a $\alpha_2\delta$-1	$Ca_v1.2$ β2a $\alpha_2\delta$-3	$Ca_v2.3$ β3	$Ca_v2.3$ β3 $\alpha_2\delta$-1	$Ca_v2.3$ β3 $\alpha_2\delta$-3
I_{Ba} density (pA/pF)	-13.8±1.4	-30.3±6.6*	-28.6±4.9*	-24.4±5.4	-98.1±20.0***	-95.4±15.6***
$V_{0.5act}$ (mV)	5.2±0.1	-5.0±0.6***	-3.5±0.5***	-13.0±1.1	-14.5±0.2	-20.1±0.7***
k_{act} (mV)	5.4±0.1	5.1±0.4	5.1±0.4	5.6±0.9	3.7±0.1	4.6±0.6
$V_{0.5inact}$ (mV)	-12.5±0.9	-19.6±0.3***	-20.5±0.4***	-64.4±0.4	-69-7±0.4***	-76.2±0.5***
k_{inact} (mV)	11.1±0.7	8.5±0.2***	8.0±0.3**	7.1±0.4	8.4±0.4*	9.5±0.4***
τ1 (ms)	273±24	260±19	156±10***	31.9±5.7	23.6±0.9	24.1±1.7
τ2 (ms)	1.16±0.08	3.54±0.46***	0.9±0.1			

Effects of the $\alpha_2\delta$-1, $\alpha_2\delta$-2a and $\alpha_2\delta$-2b subunits on the activation and inactivation of the $Ca_v1.2$/cardiac β2a calcium channel. 10mM Ba^{2+} was used as charge carrier.

	$Ca_v1.2$ β2a	$Ca_v1.2$ β2a $\alpha_2\delta$-1	$Ca_v1.2$ β2a $\alpha_2\delta$-2a	$Ca_v1.2$ β2a $\alpha_2\delta$-2b
I_{Ba} density (pA/pF)	-19.6±1.4	-57.6±8.7***	-55.8±7.5***	-50.1±4.8***
$V_{0.5act}$ (mV)	2.2±0.5	-6.2±0.7***	-7.1±0.6***	-6.1±1.1***
k_{act} (mV)	7.4±0.4	5.7±0.3**	5.2±0.3**	5.7±0.4**
$V_{0.5inact}$ (mV)	-18.3±1.3	-28.3±1.1***	-28.2±0.7***	-26.1±1.2***
k_{inact} (mV)	15.3±1.0	10.2±0.6***	9.0±0.4***	9.0±0.7***
τ1 (ms)		147.7±23.4	153.9±16.7	165.2±34.8
τ2 (ms)	796.4±185.9	1074.3±163.9	1229.1±134.7	1183.6±291.3

Effects of the $\alpha_2\delta$-1, $\alpha_2\delta$-2a and $\alpha_2\delta$-2b subunits on the activation and inactivation of the $Ca_v2.3/\beta3$ calcium channel. 10mM Ba^{2+} was used as the charge carrier.

	$Ca_v2.3$ β3	$Ca_v2.3$ β3 $\alpha_2\delta$-1	$Ca_v2.3$ β3 $\alpha_2\delta$-2a	$Ca_v2.3$ β3 $\alpha_2\delta$-2b
I_{Ba} density (pA/pF)	-40.9±4.2	-126.8±25.6**	-106.4±11.5***	-125.1±17.7***
$V_{0.5act}$(mV)	-3.1±0.5	-3.9±0.2	-12.2±0.6***	-9.1±0.4**
k_{act} (mV)	5.0±0.4	4.9±0.1	4.1±0.5	4.1±0.4
$V_{0.5inact}$ (mV)	-56.5±0.3	-61.4±0.3***	-63.2±0.4***	-62.7±0.4***
k_{inact} (mV)	7.7±0. 3	7.7±0.3	8.26±0.4	7.8±0.3
τ1(ms)	57.5±2.7	38.3±2.1***	44.3±1.6***	39.7±2.6***
τ2 (ms)	211.6±11.3	166.5±8**	217.7±17	169.3±7.3*

Effects of the $\alpha_2\delta$-1, $\alpha_2\delta$-2a and $\alpha_2\delta$-2b subunits on the activation and inactivation of the $Ca_v2.1/n\beta2a$ calcium channel. 10mM Ba^{2+} was used as the charge carrier.

	$Ca_v2.1\beta2a$	$Ca_v2.1$ nβ2a $\alpha_2\delta$-1	$Ca_v2.1$ nβ2a $\alpha_2\delta$-2	$Ca_v2.1$ nβ2a $\alpha_2\delta$-2b
I_{Ba} density (pA/pF)	-12.2±	-46.0±8.8**	-16.0±1.3*	-25.2±5.6*
$V_{0.5\ act}$ (mV)	+6.1±0.5	+6.9±0.4	+4.2±0.9	+3.0±0.8*
k_{act} (mV)	4.7±0.4	4.4±0.3	4.2±0.7	4.1±0.7
$V_{0.5inact}$ (mV)	+5.1±0.3	-6.5±0.5***	+1.0±0.3**	+0.3±0.2**
k_{inact} (mV)	5.8±0.2	6.9±0.4	6.2±0.2	6.4±0.2
τ1 (s)	1.79±0.19	1.27±0.3	1.45±0.19	1.51±0.39

Effects of the $\alpha_2\delta$-1, $\alpha_2\delta$-2a and $\alpha_2\delta$-2b subunits on the activation and inactivation of the $Ca_v3.1$ calcium channel. 10mM Ba^{2+} was used as the charge carrier.

	$Ca_v3.1$	$Ca_v3.1$ $\alpha_2\delta$-1	$Ca_v3.1$ $\alpha_2\delta$-2a	$Ca_v3.1$ $\alpha_2\delta$-2b
I_{Ba} density (pA/pF)	-62±7	-59±9	-93±15*	-72±15
$V_{0.5act}$ (mV)	-24.9±1.2	-23.4±0.7	-22.3±0.8	-21.9±0.8
k_{act} (mV)	3.9±0.3	4.3±0.2	4.1±0.2	4.2±0.3
$V_{0.5inact}$ (mV)	-54.9±1.2	-52.0±0.9	-50.4±0.7**	-50.1±0.6**
k_{inact} (mV)	4.3±0.2	4.3±0.1	4.0±0.2	4.2±0.1

Effects of co-expression of $\alpha_2\delta$-1 and -3 subunits on parameters of the current density-voltage relationship of the LVA calcium channel, $Ca_v3.1$. 20mM Ba^{2+} was used as the charge carrier.

	$Ca_v3.1$	$Ca_v3.1$ $\alpha_2\delta$-1	$Ca_v3.1$ $\alpha_2\delta$-3
V_{rev} (mV)	54.2±1.5	52.3±1.1	51.1±1.2
$V_{0.5act}$ (mV)	-28.4±0.6	-28.1±0.5	-29.8±0.5
k_{act}	4.0±0.6	4.4±0.4	4.1±0.5

8 References

Angelotti T and Hofmann F (1996) Tissue-specific expression of splice variants of the mouse voltage-gated calcium channel $\alpha_2\delta$ subunit. *FEBS Lett* **397**:331-337

Bangalore R, Mehrke G, Gingrich K, Hofmann F and Kass RS (1996). Influence of L-type Ca channel α_2/δ-subunit on ionic and gating current in transiently transfected HEK 293 cells. *Am J Physiol* **270**:H1521-H1528

Beydoun A, Uthman BM and Sackellares JC (1995) Gabapentin: Pharmacokinetics, Efficacy and Safety. *Clin Neuropharmacol* **18**:469-481

Birnbaumer L, Qin N, Olcese R, Tareilus E, Platano D, Constantin J and Stefani E. (1998) Structures and functions of calcium channel β subunits. *J Bioenerg Biomembr* **30**:357-373

Black JL and Lennon VA (1999) Identification and cloning of putative human neuronal voltage gated calcium channel γ-2 and γ-3 subunits: Neurologic implications. *Mayo Clin Proc* **74**:357-361

Brickley K, Campbell V, Berrow N, Leach R, Norman RI, Wray D, Dolphin AC and Baldwin SA (1995) Use of site-directed antibodies to probe the topography of the α_2 subunit of voltage-gated Ca^{2+} channels. *FEBS Lett* **364**:129-133

Brown JP and Gee NS (1998) Cloning and deletion mutagenesis of the $\alpha_2\delta$ calcium channel subunit from porcine cerebral cortex. *J Biol Chem* **273**:25458-25465

Brust PF, Simerson, McCue AF, Deal CR, Schoonmaker S, Williams ME, Velicelebi G, Johnson EC, Harpold MM and Ellis SB (1993) Human neuronal voltage-dependent calcium channels: studies on subunit structure and role in channel assembly. *Neuropharmacology* **32**:1089-1102

Bryans JS, Davies N, Gee NS, Dissanayake VUK, Ratcliffe GS, Horwell DC, Kneen CO, Morrell AI, Oles RJ, O'Toole JC, Perkins GM, Singh L, Sauman-Chauhan N and O'Neill JA (1998) Identification of novel ligands for the gabapentin binding site on the $\alpha_2\delta$ subunit of a calcium channel and their evaluation as anticonvulsant agents. *J Med Chem* **41**:1838-1845

Burgess DL, Davis CF, Gefrides LA and Noebels JL (1999) Identification of three novel Ca^{2+} γ subunit genes reveals molecular diversification by tandem and chromosome duplication. *Genome* **9**:1204-1213

Burgess DL, Jones JM, Meisler MH and Noebels JL (1997) Mutation of the Ca^{2+} channel β subunit Cchb4 is associated with ataxia and seizures in the lethargic (lh) mouse. *Cell* **88**:385-392

Burgess DL and Noebels JL (1999) Single gene defects in mice: the role of voltage-dependent calcium channels in absence models. *Epilepsy Res* **36**:111-122

Castellano A and Perez-Reyes (1993) Molecular diversity of Ca^{2+} channel beta subunits. *Biochem Soc Trans* **22**:483-488

Catterall WA (1998) Structure and function of neuronal Ca^{2+} channels and their role in neurotransmitter release. *Cell Calcium*. **24**:307-323

Calabresi P, Centonze, Marfia GA, Pisani A and Bernardi G (1999) An *in vitro* electrophysiological study on the effects of phenytoin, lamotrigine and gabapentin on striatal neurons. *B J Pharmacol* **126**:689-696

Chen L, Chetkovich, DM, Petralia RS, Sweeney NT, Kawasaki Y, Wenthold RJ, Bredt DS and Nicoll R (2001) Stargazin regulates synaptic targeting of AMPA receptors by two distinct mechanisms. *Nature* **408**:936-943

Craig PJ, Beattie RE, Folly EA, Banerjee MD, Reeves MB, Priestly JV, Carney SL, Sher E, Perez-Reyes E and Volsen SG (1999) Distribution of the voltage-dependent calcium channel α_{1G} subunit mRNA and protein throughout the mature rat brain. *Eur J Neurosci* **11**:2949-2964

Cribbs LL, Lee J-H, Yang J, Satin J, Zhang Y, Daud A, Barclay J, Williamson MP, Fox M, Rees M and Perez-Reyes E (1998) Cloning and characterisation of α_{1H} from human heart, a member of the T-type calcium channel gene family. *Circ Res* **83**:103-109

Curtis, MB and Catterall WA (1984) Purification of the calcium antagonist receptor of the voltage-sensitive calcium channel from skeletal muscle transverse tubules. *Biochem* **23**:2113-2118

De Jongh KS, Warner C and Catterall WA (1990) Subunits of purified calcium channels. *J Biol Chem* **265**:14738-14741

Dooley DJ, Donovan CM and Pugsley TAJ (2000) Stimulus-dependent modulation of [^{3}H]-norepinephrine release from rat neocortical slices by gabapentin and pregabalin. *Pharmacol Exp Ther* **295**:1086-93

Eberst R, Dai S, Klugbauer S and Hofmann F (1997) Identification and functional characterisation of a calcium channel gamma subunit. *Pflugers Arch* **433**:633-637

Ellis SB, Williams ME, Ways NR, Brenner R, Sharp AH, Leung AT, Campbell KP, McKenna E, Koch WJ, Hui A, Schwartz A and Harpold MM (1988) Sequence and expression of mRNAs encoding the α_1 and α_2 subunits of a DHP sensitive calcium channel. *Science* **241**:1661-1664

Felix R, Gurnett CA, De Waard M and Campbell KP (1997) Dissection of functional domains of the voltage-dependent Ca^{2+} channel $\alpha_2\delta$ subunit. *J Neurosci* **17**:6884-6891

Fink K, Meder W, Dooley DJ and Göthert M (2000) Inhibition of neuronal Ca^{2+} influx by gabapentin and subsequent reduction of neurotransmitter release from rat neocortical slices. *Brit J Pharmacol* **130**: 900-906

Freise D, Held B, Wissenbach U, Pfeifer A, Trost C, Himmerkus N, Schweig U, Freichel M, Biel M, Hofmann F, Hoth M and Flockerzi V (2000) Absence of the γ subunit of the skeletal muscle dihydropyridine receptor increases L-type Ca^{2+} currents and alters current inactivation properties. *J Biol Chem* **275**:14476-14481

Gao B, Yoshitaka S, Maximov A, Saad M, Forgacs E, Latif F, Wei MH, Lerman M, Lee J-H, Perez-Reyes E, Bezprozvanny I and Minna JD (2000) Functional properties of a new voltage-dependent calcium channel $\alpha_2\delta$ auxiliary subunit gene (CACNA2D2). *J Biol Chem* **275**:12237-12242

Gee NS, Brown JP, Dissanayake VUK, Offord J, Thurlow R and Woodruff GN (1996) The novel anticonvulsant drug, gabapentin (Neurontin) bind to the $\alpha_2\delta$ subunit of a calcium channel. *J Biol Chem* **271**:57668-5776

Gregg RG, Messing A, Strube C, Beurg M, Moss R, Behan M, Sukhareva, M, Haynes S, Powell JA, Coronado R and Powers PA (1996) Absence of the β subunit (Cchb1) of the skeletal muscle dihydropyridine receptor alters expression of the α_1 subunit and eliminates excitation-contraction coupling. *Proc Nat Acad Sci USA* **93**:13961-13966

Gurnett CA, de Waard M and Campbell KP (1996) Dual function of the voltage-dependent Ca^{2+} $\alpha_2\delta$ subunit in current stimulation and subunit interaction. *Neuron* **16**:431-440

Hill DR, Suman-Chauhan N and Woodruff GN (1993) Localisation of [^{3}H]gabapentin to a novel site in rat brain: autoradiographic studies. *Eur J Pharmacol* **244**:303-309

Hobom M., Dai S, Marais E, Lacinová L, Hofmann F and Klugbauer N (2000) Neuronal distribution and functional characterisation of the calcium channel $\alpha_2\delta$-2 subunit. *Eur J Neurosci* **12**:1217-1226

Hofmann F, Lacinová L and Klugbauer N (1999) Voltage-dependent calcium channels: from structure to function. *Rev Physiol Biochem Pharmacol* **139**:33-87

Huguenard JR (1996) Low-threshold calcium currents in central nervous system neurons. *Annu Rev Physiol* **58**:329-48

Huguenard JR (1998) Low voltage activated (T-type) calcium channel genes identified. *TINS* **21**:451452

Hullin R, Singer-Lahat D, Freichel M, Biel M, Dascal N, Hofmann F and Flockerzi V (1992) Calcium channel beta subunit heterogeneity: functional expression of cloned cDNA from heart, aorta and brain. *EMBO J* **11**:885-890

Jay SD, Ellis SB, McCue AF, Williams ME, Vedvick TS, Harpold MM and Campbell KP (1990) Primary structure of the gamma subunit of the DHP-sensitive calcium channel from skeletal muscle. *Science* **248**:490-492

Jay SD, Sharp AH, Kahl SD, Vedvick TS, Harpold MM and Campbell KP (1991) Structural characterisation of the dihydropyridine-sensitive calcium channel α_2-subunit and the associated δ peptides. *J Biol Chem* **266**:3287-3293

Klugbauer N, Dai S, Specht V, Lacinová L, Marais E, Bohn G and Hofmann F (2000). A family of calcium channel γ subunits *FEBS Lett* **470**:189-197

Klugbauer N, Lacinová L, Marais E, Hobom M and Hofmann F (1999a) Molecular Diversity of the Calcium Channel $\alpha_2\delta$ Subunit. *J Neurosci* **19**: 684-691

Klugbauer N, Marais E, Lacinová L and Hofmann F (1999b) A T-type calcium channel from mouse brain. *Pflug Arch Eur J Physiol* **437**:710-715

Lacinová L, Klugbauer N and Hofmann F (2000) Low voltage activated calcium channels: from genes to function. *Gen Physiol Biophys* **19:**121-136

Lacinová L, Klugbauer N and Hofmann F (1999) Absence of modulation of the expressed calcium channel α_{1G} by $\alpha_2\delta$ subunits. *J Physiol* **516**:639-645

Lee J-H, Daud AN, Cribbs LL, Lacerda AE, Pereverzev U, Klockner T, Schneider T and Perez-Reyes E (1999) Cloning and expression of a novel member of the low voltage activated T-type calcium channel family. *Neuroscience* **19**:1912-1921

Leiderman DB (1994) Gabapentin as add-on therapy for refractory partial epilepsy: results of five placebo controlled trials. *Epilepsia* **35**:S74-76

Ludwig A, Flockerz V and Hofmann F (1997) Regional expression and cellular localisation of the α_1 and β subunit of high voltage-activated calcium channels in rat brain *J Neurosci* **17**:1339-1349

Meder WP and Dooley DJ (2000) Modulation of K^+-induced synaptosomal calcium influx by gabapentin. *Brain Res* **875**:157-159

McLean MJ (1995) Gabapentin. *Epilepsia* **36**:S73-S86

Ng GYK, Bertrand S, Sullivan R, Ethier N, Wang J, Yergey J, Belley M, Trimble L, Bateman K, Alder L, Smith A, Mckernan R, Metters K, O'Neill GP, Lacaille JC and Herbert TE (2001) γ-Aminobutyric acid type B receptors with specific heterodimer composition and postsynaptic actions in hippocampal neurons are targets of anticonvulsant gabapentin action. *Mol Pharmacol* **59**:144-152

Perez-Reyes E, Castellano A, Kim HS, Bertrand P, Baggstrom E, Lacerda AE, Wei XY and Birnbaumer L (1992) Cloning and expression of a cardiac/brain beta subunit of the L-type calcium channel. *J Biol Chem* **267**:1792-1797

Perez-Reyes E, Cribbs LL, Daud A, Lacerda AE, Barclay J, Williamson MP, Fox M, Rees M, and Lee J-H (1998) Molecular characterization of a neuronal low-voltage-activated T-type calcium channel. *Nature* **391**:896-899

Ruth P, Röhrkasten A, Biel M, Bosse E, Regulla S, Meyer HE, Flockerzi V and Hofmann F (1988) Primary structure of the beta subunit of the DHP-sensitive calcium channel from skeletal muscle. *Science* **245**:1115-1118

Singer D, Biel M, Lotan I, Flockerzi V, Hofmann F and Dascal N (1991) The roles of the subunits in the function of the calcium channel. *Science* **253**:1553-1557

Schumacher TB, Beck H, Steinhäuser C, Schramm J and Elger CE (1998) Effects of phenytoin, carbamazepine, and gabapentin on calcium channels in hippocampal granule cells from patients with temporal lobe epilepsy. *Epilepsia* **39**:355-363

Soong TW, Stea A, Hodson CD, Dubel SJ, Vincent SR and Snutch TP (1993) Structure and functional expression of a member of the low voltage activated calcium channel family. *Science* **260**:1133-1136

Stefani A, Spadoni F and Bernardi G (1998) Gabapentin inhibits calcium currents in isolated rat brain neurons. *Neuropharmacology* **37**:83-91

Suh-Kim H, Wei X, Klos A, Pan S, Ruth P, Flockerzi V, Hofmann F, Perez-Reyes E and Birnbaumer L (1996) Reconstitution of the skeletal muscle dihydropyridine receptor: functional interaction among α_1, β, γ and $\alpha_2\delta$ subunits. *Receptor and Channels* **4**:217-225

Suman-Chauhan N, Webdale L, Hill DR and Woodruff GN (1993) Characterisation of [^{3}H]gabapentin binding to a novel site in rat brain: homogenate binding studies. *Eur J Pharmacol* **244**:293-301

Talley EM, Cribbs LL, Lee J-H, Daud A, Perez-Peyes E and Bayliss DA (1999) Differential distribution of a gene family encoding low voltage-activated (T-type) calcium channels. *J Neurosci* **19** :1895-1911

Taylor CP, Gee NS, Su T-Z, Kocsis JD, Welty DF, Brown JP, Dooley, Boden P and Singh L (1998) A summary of mechanistic hypotheses of gabapentin pharmacology. *Epilepsy Res* **29**:233-249

Taylor CP, Vartanian MG, Yuen P-W, Bigge C, Suman-Chauhan N and Hill DR (1993) Potent and stereospecific anticonvulsant activity of 3-isobutyl GABA relates to in vitro binding at a novel site labeled by tritiated gabapentin. *Epilepsy Res* **14**:11-15

Taylor MT and Bonhaus DW (2000) Allosteric modulation of [^{3}H]gabapentin binding by ruthenium red. *Neuropharmacology* **39**:1267-1273

Wang M, Offord J, Oxender DL and Su T-Z (1999) Structural requirement of the calcium-channel subunit $\alpha_2\delta$ for gabapentin binding. *Biochem J* **342**: 313-320

Welty DF, Schielke GP, Vartanian MG and Taylor CP (1993) Gabapentin anticonvulsant action in rats: disequilibrium with peak drug concentrations in plasma and brain microdialysate. *Epilepsy Res* **16**:175-181

Westenbroek RF, Hell JW, Warner C, Dubel SJ, Snutch TP and Caterrall WA (1992) Biochemical properties and subcellular distribution of an N-type calcium channel α1 subunit. *Neuron* **9**:1099-1115

Westenbroek RE, Sakurai T, Elliott EM, Hell JW, Starr TV, Snutch TP and Catterall WA (1995) Immunochemical identification and subcellular distribution of the α_{1A} subunits of brain calcium channels *J Neurosci* **15**:6403-6418

Wiser O, Trus M, Tobi D, Halevi S, Giladi E and Atlas D (1996) The α_2/δ subunit of voltage sensitive Ca^{2+} channels is a single transmembrane extracellular protein which is involved in regulated secretion. *FEBS Lett* **379**:15-20

Yamaguchi H, Okuda M, Mikala G, Fukasawa K and Varadi G (2000) Cloning of the β_{2a} subunit of the voltage dependent calcium channel from human heart: cooperative effect of α_2/δ and β_{2a} on the membrane expression of the α_{1C} subunit. *Biochem Bioph Res Co* **267**:156-163

8.1 Own Publications

Marais E, Klugbauer N and Hofmann F (2001) Calcium Channel $\alpha_2\delta$ Subunits – Structure and Gabapentin Binding *Mol Pharmacol* **59**:1243-1248

Klugbauer N, Dai S, Specht V, Lacinová L, Marais E, Bohn G and Hofmann F (2000). A family of calcium channel γ subunits *FEBS Lett* **470**:189-197

Klugbauer N, Lacinová L, Marais E, Hobom M and Hofmann F (1999) Molecular Diversity of the Calcium Channel $\alpha_2\delta$ Subunit. *J Neurosci* **19**: 684-691

Klugbauer N, Marais E, Lacinová L and Hofmann F (1999) A T-type calcium channel from mouse brain. *Pflug Arch Eur J Physiol* **437**:710-715

Hobom M, Dai S, Marais E, Lacinová L, Hofmann F and Klugbauer N (1999) Neuronal distribution and functional characterisation of the calcium channel $\alpha_2\delta$-2 subunit. *Eur J Neurosci* **12**:1217-1226

9 Acknowledgements

I would like to thank the following people whose assistance was of inestimable value to me:

Prof. Dr. Franz Hofmann and PD Dr. Norbert Klugbauer who supervised this work. Without their vision, guidance and support, this work would not have been possible.

Prof. Dr. W. Staudenbauer for being my doctor father.

Dr. Lubica Lacinová, who performed most of the electrophysiological experiments in this thesis and was always available to explain principles and results.

Dr. Shui-ping Dai who performed some of the $\alpha_2\delta$-2a, $\alpha_2\delta$-2b and γ subunit electrophysiological measurements

Drs. Andrea Gerstner, Claudia Seisenberger and Verena Specht who showed me the ropes in the lab.

Dr. Jens Schlossman, whose expertise in protein techniques and clarity of thinking were indispensible.

Susanne Kampf, Anna Klein and Sabine Ehrhardt whose technical and personal assistance were invaluable in the laboratory.

Dr. Sven Godorr for a critical review of this manuscript.

The organisers and members of the Graduiertenkolleg 333, through which my scientific knowledge outside of this thesis was expanded and enriched. In particular I acknowledge the assistance of Dr. Martina Haaseman, whose ever-friendly help in matters organisatorial and otherwise is much appreciated.

I gratefully acknowledge the support of the National Research Foundation of South Africa and the Emily Fuchs Foundation, which enabled me to travel to, and study in, Germany.

I thank everyone at the Institut für Pharmakologie und Toxikologie der Technischen Universität München for their help and friendliness.